

Cosmic ray physics in calculations of cosmological structure formation

T. A. Enßlin¹, C. Pfrommer^{1,2}, V. Springel¹, and M. Jubelgas¹

- ¹ Max-Planck-Institut für Astrophysik, Karl-Schwarzschild-Str.1, PO Box 1317, 85741 Garching, Germany
e-mail: ensslin@mpa-garching.mpg.de (TAE); volker@mpa-garching.mpg.de (VS); martin.jubelgas@gmail.com (MJ)
- ² Canadian Institute for Theoretical Astrophysics, University of Toronto, 60 St. George Street, Toronto, Ontario, M5S 3H8, Canada
e-mail: pfrommer@cita.utoronto.ca

Preprint online version: July 18, 2021

ABSTRACT

Cosmic rays (CRs) play a decisive role within our own Galaxy. They provide partial pressure support against gravity, they trace past energetic events such as supernovae, and they reveal the underlying structure of the baryonic matter distribution through their interactions. To study the impact of CRs on galaxy and cosmic structure formation and evolution, we develop an approximative framework for treating dynamical and radiative effects of CRs in cosmological simulations. Our guiding principle is to try to find a balance between capturing as many physical properties of CR populations as possible while at the same time requiring as little extra computational resources as possible. We approximate the CR spectrum of each fluid element by a single power-law, with spatially and temporally varying normalisation, low-energy cut-off, and spectral index. Principles of conservation of particle number, energy, and pressure are then used to derive evolution equations for the basic variables describing the CR spectrum, both due to adiabatic and non-adiabatic processes. The processes considered include compression and rarefaction, CR injection via shocks in supernova remnants, injection in structure formation shock waves, in-situ re-acceleration of CRs, CR spatial diffusion, CR energy losses due to Coulomb interactions, ionisation losses, Bremsstrahlung losses, and, finally, hadronic interactions with the background gas, including the associated γ -ray and radio emission due to subsequent pion decay. We show that the formalism reproduces CR energy densities, pressure, and cooling rates with an accuracy of $\sim 10\%$ in steady state conditions where CR injection balances cooling. It is therefore a promising formulation to allow simulations where CR physics is included. Finally, we briefly discuss how the formalism can be included in Lagrangian simulation methods such as the smoothed particle hydrodynamics technique. Our framework is therefore well suited to be included into numerical simulation schemes of galaxy and structure formation.

Key words. Cosmic rays – galaxies: ISM – intergalactic medium – galaxies: cluster: general – acceleration of particles – radiation mechanisms: non-thermal

1. Introduction

1.1. Motivation

The interstellar medium (ISM) of galaxies is highly complex, with an energy budget composed both of thermal and non-thermal components. Each of the non-thermal components which are magnetic fields and cosmic rays (CRs) are known to contribute roughly as much energy and pressure to the ISM as the thermal gas does, at least in our own Galaxy.

Magnetic fields permeate the ISM and seem to have ordered and turbulent field components. Very likely they play an important role in moderating molecular cloud collapse and star formation. They are the ISM ingredient which couples otherwise dynamically independent ingredients like the ISM plasma, the CR gas, and (charged) dust particles into a single, however complex fluid.

CRs behave quite differently compared to the thermal gas. Their equation of state is softer, they are able to travel actively over macroscopic distances, and their energy loss time-scales are typically larger than the thermal ones. Furthermore, roughly half of their energy losses are due to Coulomb and ionisation interactions and thereby heat the thermal gas. Therefore, CR

populations are an important galactic storage for energy from supernova explosions, and thereby help to maintain dynamical feedback of star formation for periods longer than thermal gas physics alone would permit. The spectral distribution of CRs is much broader than that of thermal populations, which has to be taken into account in estimating their dynamical properties. The dynamical important part of CR spectral distributions in momentum spaces easily encompasses a few orders of magnitude, whereas thermal distributions appear nearly mono-energetic on logarithmic scales (see Fig. 1).

Numerical simulations and semi-analytical models of galaxy and large-scale structure formation neglected the effects of CRs and magnetic fields so far, despite their dynamical importance. Although there have been attempts to equip SPH galaxy formation codes with magnetic field descriptions on the MHD level (Dolag et al. 1999), a fully dynamical treatment of the CR component has not yet been attempted due to the very complex CR physics involved. There have been pioneering efforts to furnish grid-based MHD codes with a diffusive CR component in order to study isolated effects like Parker instabilities (Kuwabara et al. 2004; Hanasz & Lesch 2003) or the injection of CRs into the wider IGM (Miniati et al. 2001; Ryu et al. 2003; Ryu & Kang 2003, 2004) and ISM (Snodin et al. 2006). However, these codes are not suited for galaxy formation simulations in a cosmologi-

cal setting due to the missing adaptive resolution capability, and the lack of a treatment of cosmological components such as dark matter and stellar populations. There have also been numerical implementations of discretised CR energy spectra on top of grid-based cosmological simulations (Miniati 2001), but these implementations neglected the hydrodynamic pressure of the CR component. In addition, the amount of computer resources required for these models in terms of memory and CPU-time is substantial. This renders this approach unattractive for self-consistent simulations of galaxy formation and inhibits the inclusion of CRs into cosmological simulations of structure formation, where it is not clear *ab initio* if CRs are crucial or not.

An accurate description of CRs should follow the evolution of the spectral energy distribution of CRs as a function of time and space, and keep track of their dynamical, non-linear coupling with the hydrodynamics. In order to allow the inclusion of CRs and their effects into numerical simulations and semi-analytic descriptions of galaxy formation, we develop a simplified description of the CR dynamics and physics. We seek a compromise between two opposite requirements, namely: (i) to capture as many physical properties and peculiarities of CR populations as possible, and (ii) to require as little extra computational resources as possible. In our model, the emphasis is given to the dynamical impact of CRs on hydrodynamics, and not on an accurate spectral representation of the CRs. The guiding principles are energy, pressure, and particle number conservations, as well as adiabatic invariants. Non-adiabatic processes will be mapped onto modifications of these principles.

The goal of the formalism is to permit explorative studies investigating under which circumstances CRs are likely to affect galactic or cosmic structure formation processes. The approach is phenomenological, which implies that any adopted model parameter like CR injection efficiency or diffusivity has to be verified by independent means before definite conclusions may be drawn, if the conclusions depend strongly on those assumptions. Nevertheless, it is plausible that in many cases the overall physical picture will not sensitively depend on the details of the CR description, but merely on the presence of CRs. An implementation of the formalism in a cosmic structure formation code will therefore allow an identification of regimes in which CRs are likely to have a significant impact on the properties of galaxies and galaxy clusters. We want to stress that including “only” an approximate description of CR dynamics into galaxy and structure formation calculations should be regarded as a significant improvement compared to the current situation where the CRs are ignored completely.

In this paper, we give the theoretical basis and justification of our formalism. An implementation and first applications of our formalism are described by two companion papers. Jubelgas et al. (2006) describe the implementation into the GADGET code and present first results on galaxy formation including CRs. Pfrommer et al. (2006) develop a SPH Mach number measuring scheme, which is a necessary prerequisite to study CRs injected at accretion shock waves in the cosmic large-scale structure.

1.2. Approximations and assumptions

A number of simplifying assumptions are necessary in order to reduce the large number of degrees of freedom of a CR population before it can be included in a numerical tractable scheme. For transparency, we list the main assumptions here:

1. **Protons dominate the CR population:** We only model the dominant CR proton population, assuming that the presence

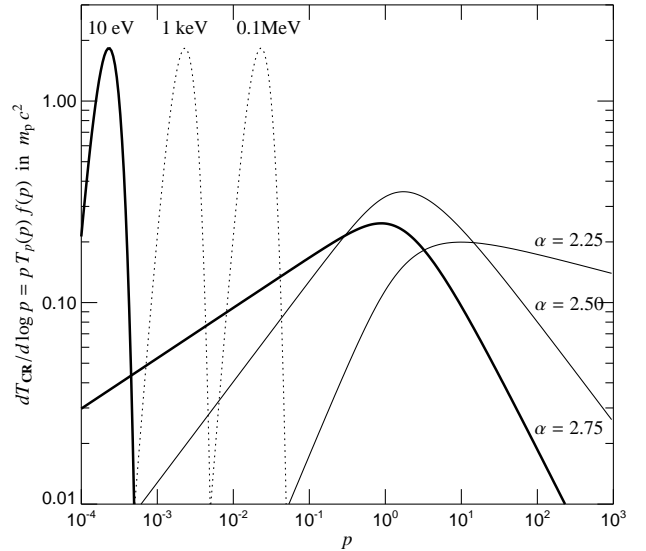


Fig. 1. Thermal and power-law (CR) proton spectra for a variety of temperatures and spectral indices α . No low momentum cutoff was imposed onto the CR populations. Displayed is the energy per logarithmic momentum interval over dimensionless proton momenta $p = P_p/(m_p c^2)$. This form of presentation permits to read-off the dynamically important momentum ranges of the populations. All spectra are normalised to exhibit the same pressure. The thick lines represents a possible location in the hot medium of our Galaxy ($kT = 10$ eV, $\alpha = 2.75$) where thermal equals CR pressure. The break in the CR energy distributions is solely due to the change in the kinetic energy formulae in the trans-relativistic regime.

of α -particles and heavier ions would not change the dynamical picture. In contrast to heavier ions, α -particles carry a significant fraction of the total CR energy. Nevertheless, our assumption is a reasonable approximation, since the energy density of α -particles can be absorbed into the proton spectrum. As a coarse approximation, a GeV energy α -particle can be regarded as an ensemble of four individual nucleons traveling together due to the relatively weak MeV nuclear binding energies compared to the kinetic energy of relativistic protons. For hadronic interactions, the fact that the four nucleons are bound is of minor importance. Since Coulomb cooling and ionisation losses are proportional to the square of the nucleus' charge, each of the four nucleons of the α -particle is experiencing a loss of kinetic energy which is identical to the loss that a free CR proton with exactly the same specific energy would experience. Furthermore, due to their low galactic energy density, but also due to their more complex radiative losses, we ignore CR electron populations. Only a description of quasi-equilibrium secondary electrons resulting from hadronic CR-gas interactions is provided, which has some restricted applicability in galaxy cluster physics.

2. **A momentum power-law is a typical spectrum:** We assume that the CR momentum spectrum can be well described by a power-law with spectral index α . This is not only consistent with the observation of Galactic CRs ($\alpha \approx 2.75$) but is also predicted by many CR acceleration and diffusion models, which frequently give momentum power-law spectra (see Schlickeiser 2002, for a review). Especially CR injection at shock waves in the test-particle limit predicts power-law spectra in momentum space. The dynamically rel-

evant physical quantities of the CR population are its kinetic energy density ε_{CR} , the average energy $T_{\text{CR}} = \varepsilon_{\text{CR}}/n_{\text{CR}}$, and the pressure P_{CR} . For an assumed power-law spectrum with steep spectral index α at high CR momenta, these two quantities are completely determined by a specification of the normalisation constant C and the low-momentum cutoff q of the power-law. No high-momentum cutoff of the spectrum is considered, since for a sufficiently steep spectrum ($\alpha > 2$), the high-energy range is dynamically unimportant. Instead, the dynamics is dominated by particles with momenta closest to $q m_p c$ (the particles at the lower cutoff), or around $m_p c$, whichever is larger (and the latter only if $\alpha < 3$, otherwise the particles at $q m_p c$ dominate always).

3. **Energy, particle number, and pressure are the relevant CR variables:** The many degrees of freedom a CR spectrum have to be reduced to simplified evolution equations for the spectral normalisation constant C , for the cutoff q , and eventually for the spectral index α . The mapping of the full spectral dynamics on this restricted set of variables is not unique. However, physical intuition tells us that the most relevant quantities, which should be reproduced in the formalism with highest accuracy, are the CR energy density, the number density, and the pressure. CR pressure, which is very similar to the CR energy density, will only be used if a varying spectral index is chosen. Therefore, whenever a physical effect modifies a CR spectrum, the changes on C , q , and eventually α will be calculated by taking energy, particle and eventually pressure conservation into account. Whenever we have to make a choice we will favour accuracy in CR energy over accuracy in CR number density. This choice is motivated by our aim to study the dynamical effects of a CR population on their host environment. Spectral details of the CR populations, which are not the focus of our formalism, are therefore treated very coarsely.

We present two models for the description of the CR population that differ in the degree of their complexity. In the simpler model, we assume the CR spectral index α to be the same everywhere, while in the more complex model we allow it to vary in space and time. The model with the constant spectral index suppresses a number of CR phenomena like spectral steepening due to transport effects, or spectral flattening due to fresh particle injection. However, these effects are probably not essential for a first order description of the global dynamical impact of CRs.

1.3. Captured physics

Our framework is set up to accommodate a number of essential physical processes of CR gases, like particle acceleration, diffusion, and particle interactions. The different components of our framework are of different relevance in the various astrophysical environments:

1. CR energy is an important energy storage within galactic metabolisms. In our Galaxy, the CR energy density is comparable to the thermal one.
2. CR pressure is suspected to play an important role in forming galactic winds.
3. Adiabatic energy losses and gains of CRs are the mechanical way to exchange energy with the thermal gas, and therefore relevant for CR driven winds or radio bubbles in cluster atmospheres.
4. Shock acceleration is believed to be an important source of CRs. In the galactic context, supernova shock waves should

dominate the energy injection, in galaxy clusters, the cluster merger and accretion shock waves may be more efficient.

5. The role of CR diffusion is actually not always clear. Diffusive escape times in galaxy clusters exceed the Hubble time for GeV particles, whereas we know that CRs escape from our own galaxy on time-scales of 10^7 years, which certainly involves diffusive CR transport.
6. In situ CR re-acceleration by plasma waves may energise relativistic electrons in several astrophysical environments. This process may be important for cluster radio halos but also in several other astrophysical situations (Galaxy, Sun,...).
7. Coulomb and ionisation energy losses of the CRs are heating the gas, thereby possibly maintaining a minimum temperature and ionisation in dense molecular clouds.
8. Bremsstrahlung from CR protons is not an important effect – to our knowledge –, neither for the CR cooling, nor for the production of high-energy photons.
9. Hadronic interactions is the only efficient non-adiabatic energy loss process of ultra-relativistic protons. Their secondaries (photons, electrons) are important tracers of CR populations. Gamma rays from such interactions are observed from our Galaxy. In galaxy clusters, synchrotron emission of secondary electrons is proposed as a possible origin of the giant radio halos (among other possibilities, see point 6).

Thus, these effects should allow realistic studies of the impact of a variety of physical processes of CRs on galaxies, clusters of galaxies, and on the large-scale intergalactic medium, including:

1. hydrodynamical effects of CRs,
2. CR injection by diffusive shock acceleration,
3. in-situ re-acceleration by plasma waves,
4. non-local feedback from CR injection due to CR diffusion,
5. CR modified shock structures,
6. heating of cold gas by CRs,
7. CR driven galactic winds,
8. Parker instabilities of spiral galaxy disks,
9. rough morphology of gamma ray emission,
10. rough morphology of radio emission due to secondary electrons.

We like to point out that our approach is a phenomenological one which does not provide first principle descriptions of the above physical effects. It is also not always accurate, especially when spectral effects become relevant and deviations from power-law spectra are expected, e.g. in the case of non-linear shock acceleration. Although our formalism captures many properties only approximately, it allows to study many astrophysical consequences in greater detail than before and also permits to study the influence of the adopted CR parameters like injection efficiency, diffusivity, etc. on observable quantities.

1.4. Structure of paper

Our basic formalism is outlined in Sect. 2, in which the approximative description of the CR gas is introduced and its adiabatic evolution is described (Sect. 2.1). A model with a constant spectral index for the power-law description of the CR population is given in Sect. 2.2 while the more general approach with a spatially and temporally varying spectral index is presented in Sect. 2.3. Sect. 3 contains the technical description of the various non-adiabatic processes: CR injection via shocks waves of structure formation (Sect. 3.1.1), and of supernova remnants (Sect. 3.1.2); CR spatial diffusion (Sect. 3.2); in-

situ re-acceleration of CRs (Sect. 3.3); CR energy losses due to Coulomb interactions (Sect. 3.4), ionisation losses (Sect. 3.5), Bremsstrahlung (Sect. 3.6), and hadronic interactions with the background gas (Sect. 3.7), including the associated γ -radiation from the π^0 -decays (Sect. 3.8) and the radio emission of the electrons and positrons resulting from π^\pm -decays (Sect. 3.9). Steady state CR spectra, for which injection and cooling balance each other, and freely cooling CR spectra are calculated exactly and with our formalism are compared in Sect. 4. Section 5 describes how the formalism can be included into a simulation code based on smoothed particle hydrodynamics (SPH). Finally, we give our conclusions in Sect. 6.

2. Formalism

In this section, we develop a description of a CR population in a volume element which is comoving with the background fluid. This Lagrangian perspective results in a significant simplification, since the advective transport processes are fully characterised by a description of the effects of adiabatic volume changes. We will introduce convenient, adiabatically invariant variables which are constant in time in the absence of non-adiabatic processes. When non-adiabatic processes are included, they can be expressed in terms of evolutionary equations for the adiabatically invariant variables. The chosen formalism is well suited for the implementation in Lagrangian numerical simulation codes, as will be discussed in more detail in Sect. 5 for the example of SPH codes.

2.1. Basic cosmic ray variables

Since we only consider CR protons, which are at least in our Galaxy the dominant CR species, it is convenient to introduce the dimensionless momentum $p = P_p/(m_p c)$. We assume that the differential particle momentum spectrum per volume element can be approximated by a single power-law above the minimum momentum q :

$$f(p) = \frac{dN}{dp dV} = C p^{-\alpha} \theta(p - q), \quad (1)$$

where $\theta(x)$ denotes the Heaviside step function. Note that we use an effective one-dimensional distribution function $f(p) \equiv 4\pi p^2 f^{(3)}(p)$. The differential CR spectrum can vary spatially and temporally (although for brevity we suppress this in our notation) through the spatial dependence of the normalisation $C = C(\mathbf{x}, t)$ and the cutoff $q = q(\mathbf{x}, t)$. In the simpler of our two models, we assume the CR spectral index α to be constant in space and time, while the more complex model allows for a spatial and temporal variation of α as well.

Adiabatic compression or expansion leaves the phase-space density of the CR population invariant, leading to a momentum shift according to $p_0 \rightarrow p = (\rho/\rho_0)^{1/3} p_0$ for a change in density from ρ_0 to ρ . Since this is fully reversible, it is useful to introduce an invariant cutoff q_0 and a normalisation C_0 which describe the CR population via Eqn. (1) if the gas is adiabatically compressed or expanded relative to the reference density ρ_0 . The actual parameters of the spectrum are then given by

$$q(\rho) = (\rho/\rho_0)^{1/3} q_0 \quad \text{and} \quad C(\rho) = (\rho/\rho_0)^{\frac{\alpha+2}{3}} C_0. \quad (2)$$

The variables q_0 and C_0 are hence a convenient choice for a Lagrangian description of the ISM or the intra-cluster medium (ICM).

The CR number density is given by

$$n_{\text{CR}} = \int_0^\infty dp f(p) = \frac{C q^{1-\alpha}}{\alpha-1} = \frac{C_0 q_0^{1-\alpha}}{\alpha-1} \frac{\rho}{\rho_0}, \quad (3)$$

provided $\alpha > 1$. The kinetic energy density of the CR population is

$$\varepsilon_{\text{CR}} = \int_0^\infty dp f(p) T_p(p) = \frac{C m_p c^2}{\alpha-1} \times \left[\frac{1}{2} \mathcal{B}_{\frac{1}{1+q^2}} \left(\frac{\alpha-2}{2}, \frac{3-\alpha}{2} \right) + q^{1-\alpha} \left(\sqrt{1+q^2} - 1 \right) \right], \quad (4)$$

where $T_p(p) = (\sqrt{1+p^2} - 1) m_p c^2$ is the kinetic energy of a proton with momentum p . $\mathcal{B}_x(a, b)$ denotes the incomplete Beta-function, and $\alpha > 2$ is assumed. The average CR kinetic energy $T_{\text{CR}} = \varepsilon_{\text{CR}}/n_{\text{CR}}$ is therefore

$$T_{\text{CR}} = \left[\frac{q^{\alpha-1}}{2} \mathcal{B}_{\frac{1}{1+q^2}} \left(\frac{\alpha-2}{2}, \frac{3-\alpha}{2} \right) + \sqrt{1+q^2} - 1 \right] m_p c^2. \quad (5)$$

The CR pressure is

$$P_{\text{CR}} = \frac{m_p c^2}{3} \int_0^\infty dp f(p) \beta p = \frac{C m_p c^2}{6} \mathcal{B}_{\frac{1}{1+q^2}} \left(\frac{\alpha-2}{2}, \frac{3-\alpha}{2} \right), \quad (6)$$

where $\beta = v/c = p/\sqrt{1+p^2}$ is the dimensionless velocity of the CR particle. The CR population can hydrodynamically be described by an isotropic pressure component as long as the CRs are coupled to the thermal gas by small scale chaotic magnetic fields. Note, that for $2 < \alpha < 3$ the kinetic energy density and pressure of the CR populations are well defined for the limit $q \rightarrow 0$, although the total CR number density diverges.

The local adiabatic exponent of the CR population is defined by

$$\gamma_{\text{CR}} \equiv \left. \frac{d \log P_{\text{CR}}}{d \log \rho} \right|_S, \quad (7)$$

where the derivative has to be taken at constant entropy S . Using Eqns. (2) and (6), we obtain for the CR adiabatic exponent

$$\begin{aligned} \gamma_{\text{CR}} &= \frac{\rho}{P_{\text{CR}}} \left(\frac{\partial P_{\text{CR}}}{\partial C} \frac{\partial C}{\partial \rho} + \frac{\partial P_{\text{CR}}}{\partial q} \frac{\partial q}{\partial \rho} \right) \\ &= \frac{\alpha+2}{3} - \frac{2}{3} q^{2-\alpha} \beta(q) \left[\mathcal{B}_{\frac{1}{1+q^2}} \left(\frac{\alpha-2}{2}, \frac{3-\alpha}{2} \right) \right]^{-1}. \end{aligned} \quad (8)$$

Note that the CR adiabatic exponent is time dependent due to its dependence on the lower cutoff of the CR population, q , which is shown in Fig. 2. For a mixture of thermal and CR gas, it is appropriate to define an effective adiabatic index by

$$\gamma_{\text{eff}} \equiv \left. \frac{d \log(P_{\text{th}} + P_{\text{CR}})}{d \log \rho} \right|_S = \frac{\gamma_{\text{th}} P_{\text{th}} + \gamma_{\text{CR}} P_{\text{CR}}}{P_{\text{th}} + P_{\text{CR}}}. \quad (9)$$

2.2. Formalism with a constant spectral index

The spectrum of the CR population within a given fluid element is shaped by a number of different physical processes, such as particle injection and escape, continuous and hadronic energy losses, or re-acceleration. While all of these processes leave a characteristic signature in the CR spectrum, in the framework of our simplified model we have to describe their effects in terms of the two dynamical variables, C and q (or C_0 and q_0). In order to

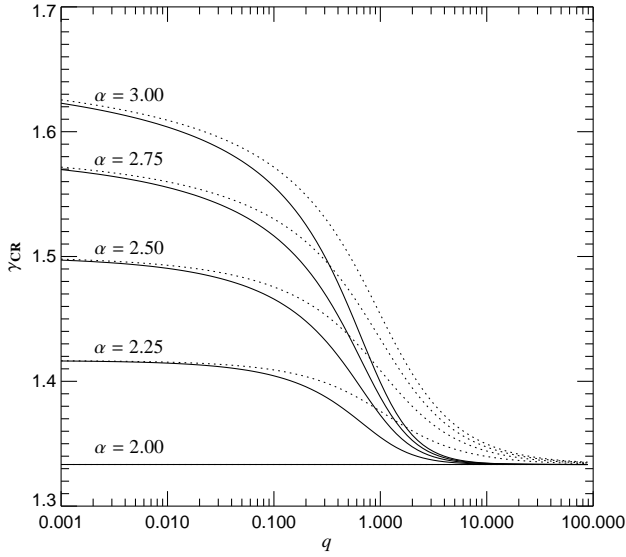


Fig. 2. Adiabatic index γ_{CR} of a CR population as a function of the lower momentum cutoff q for a variety of spectral indices α (solid lines). Furthermore, the pseudo-adiabatic index $\gamma_{\text{CR}}^* = 1 + P_{\text{CR}}/\epsilon_{\text{CR}}$ relating the total CR pressure and energy density is also displayed (dotted lines). Only for a polytropic gas behaviour we have $\gamma_{\text{CR}} = \gamma_{\text{CR}}^*$. This applies approximately for CR populations which are either completely non- or completely ultra-relativistic. However, in the here important case of trans-relativistic CR populations polytropic equations of state can not be assumed.

approximate the key features of the real CR dynamics with our description, we have to make a proper choice for how to modify our variables by the different processes. The guiding principle for this are energy and particle number conservation.

Consider a non-adiabatic process leading to a change dn_{CR} in the number density and a change $d\epsilon_{\text{CR}}$ in the energy density of the particles during an infinitesimal time interval dt . The implied change in (C, q) is then given by

$$\begin{pmatrix} dC \\ dq \end{pmatrix} = \begin{pmatrix} \partial C/\partial n_{\text{CR}} & \partial C/\partial \epsilon_{\text{CR}} \\ \partial q/\partial n_{\text{CR}} & \partial q/\partial \epsilon_{\text{CR}} \end{pmatrix} \begin{pmatrix} dn_{\text{CR}} \\ d\epsilon_{\text{CR}} \end{pmatrix}. \quad (10)$$

The inverse of the Jacobian can be straight forwardly calculated using the definitions in Eqns. (3) and (4) which can easily be inverted to yield

$$dC = C \frac{d\epsilon_{\text{CR}} - T_p(q) dn_{\text{CR}}}{\epsilon_{\text{CR}} - T_p(q) n_{\text{CR}}}, \quad (11)$$

$$dq = \frac{q}{\alpha - 1} \frac{d\epsilon_{\text{CR}} - T_p(q) dn_{\text{CR}}}{\epsilon_{\text{CR}} - T_p(q) n_{\text{CR}}}. \quad (12)$$

These relations are reasonable, which can also be verified by the following gedanken experiments: if a process increases ϵ_{CR} and n_{CR} simultaneously by the same factor $1 + \delta$, so that $d\epsilon_{\text{CR}}/\epsilon_{\text{CR}} = dn_{\text{CR}}/n_{\text{CR}} = \delta$, one gets only a change in the normalisation ($dC = \delta C$), but not in the cutoff ($dq = 0$), as it should be. If one adds an infinitesimal amount of particles dn_{CR} with exactly the kinetic energy of the cutoff $T_p(q)$, so that $d\epsilon_{\text{CR}} = T_p(q) dn_{\text{CR}}$, the normalisation is unchanged ($dC = 0$), but the cutoff is lowered ($dq = -q dn_{\text{CR}}/[(\alpha - 1) n_{\text{CR}}] \Rightarrow n_{\text{CR}} \propto q^{1-\alpha}$), again as expected.

The adiabatically invariant variables change according to

$$dC_0 = \left(\frac{\rho}{\rho_0}\right)^{-\frac{\alpha+2}{3}} dC = C_0 \frac{d\epsilon_{\text{CR}} - T_p(q) dn_{\text{CR}}}{\epsilon_{\text{CR}} - T_p(q) n_{\text{CR}}}, \quad (13)$$

$$dq_0 = \left(\frac{\rho}{\rho_0}\right)^{-\frac{1}{3}} dq = \frac{q_0}{\alpha - 1} \frac{d\epsilon_{\text{CR}} - T_p(q) dn_{\text{CR}}}{\epsilon_{\text{CR}} - T_p(q) n_{\text{CR}}}, \quad (14)$$

where we used a notation which is mixed in the variant and invariant variables, for convenience. Ways to numerically implement the evolution of C_0 and q_0 are discussed in Appendix A.1.

2.3. Formalism with a variable spectral index

The modeling of certain effects of CR physics such as spectral steepening due to transport effects, or spectral flattening due to fresh particle injection requires a more elaborate description of the CR population. Thus, we generalise the above formalism by allowing the spectral index to vary in space and time as well. To this end, we now consider the CR population to be described by three dynamical variables C , q , and α . In addition to energy and particle number conservation, we invoke pressure conservation. As a word of caution, we note that the resulting formalism is considerably more demanding in terms of computational resources than the formulation with a constant spectral index. We hence suggest that this description is only used if the problem under consideration requires this additional information.

For notational purposes, we define a three-vector with the dynamical CR variables as $\mathbf{a} \equiv (C, q, \alpha)^T$, where the exponent denotes the transpose of the vector. Similarly, we define a vector of hydrodynamic CR quantities $\mathbf{h} \equiv (n_{\text{CR}}, \epsilon_{\text{CR}}, P_{\text{CR}})^T$. Consider a non-adiabatic process leading to an infinitesimal change dn_{CR} in the number density, $d\epsilon_{\text{CR}}$ in the energy density, and dP_{CR} in the pressure of the particles during an infinitesimal time interval dt . This implies a change in $\mathbf{a} = (C, q, \alpha)^T$ given by

$$da_i = \sum_{j=1}^3 \frac{\partial a_i}{\partial h_j} dh_j \Leftrightarrow d\mathbf{a} = \mathbf{A} d\mathbf{h}. \quad (15)$$

Since the entries of the Jacobian \mathbf{A} cannot be straightforwardly obtained, we propose to compute them by inverting the inverse of the Jacobian \mathbf{A}^{-1} . Once this is achieved, the changes $d\mathbf{a}$ in the dynamical CR variables can be easily obtained. The inverse of the Jacobian is given by

$$\mathbf{A}^{-1} = \begin{pmatrix} \frac{n_{\text{CR}}}{C} & -\frac{\alpha-1}{q} n_{\text{CR}} & \frac{\partial n_{\text{CR}}}{\partial \alpha} \\ \frac{\epsilon_{\text{CR}}}{C} & -\frac{\alpha-1}{q} n_{\text{CR}} T_p(q) & \frac{\partial \epsilon_{\text{CR}}}{\partial \alpha} \\ \frac{P_{\text{CR}}}{C} & -\frac{m_p c^2 (\alpha-1)}{3} \beta(q) n_{\text{CR}} & \frac{\partial P_{\text{CR}}}{\partial \alpha} \end{pmatrix}, \quad (16)$$

where the last column can be explicitly expressed as

$$\frac{\partial n_{\text{CR}}}{\partial \alpha} = -\frac{n_{\text{CR}}}{\alpha-1} [1 + (\alpha-1) \ln q], \quad (17)$$

$$\frac{\partial \epsilon_{\text{CR}}}{\partial \alpha} = -\int_0^\infty dp T_p(p) f(p) \ln p, \quad (18)$$

$$\frac{\partial P_{\text{CR}}}{\partial \alpha} = -\frac{m_p c^2}{3} \int_0^\infty dp p \beta(p) f(p) \ln p. \quad (19)$$

We discuss ways to numerically implement the time evolution of C_0 , q_0 , and α in Appendix A.2.

A note of caution should be in order. For ultra-relativistic CR populations the formalism with varying spectral index becomes degenerate, since in this regimes the equation of state is independent of the spectral index (see Fig. 2). However, as can be seen in Sect. 4, the dynamics of CR cooling always pushes the low-energy cutoff into the trans-relativistic regime, where this formalism should work.

3. Non-adiabatic processes

In the following, we discuss various non-adiabatic source and sink processes of the CR population. In each subsection, we outline the physical motivation of each process and describe its effects in terms of a change in energy and number density. Afterwards, we generalise to the more complex case of a spatially and temporally varying CR spectral index.

3.1. CR shock acceleration

In this section, we discuss CR acceleration processes at shock waves due to gas accretion and galaxy mergers, using the framework of *diffusive shock acceleration*. Our description is a modification of the approach of Miniati (2001). The shock surface separates two regions: the *upstream regime* defines the region in front of the shock which is causally unconnected for super sonic shock waves, whereas the *downstream regime* lies in the wake of the shock wave. The shock front itself is the region in which the mean plasma velocity changes rapidly on small scales, governed by plasma physics. In the rest frame of the shock, particles are impinging onto the shock surface at a rate per unit area of $\rho_2 v_2 = \rho_1 v_1$. Here v_1 and v_2 give the plasma velocities (relative to the shock's rest frame) in the upstream and downstream regimes of the shock, respectively. The corresponding mass densities are denoted by ρ_1 and ρ_2 .

We assume that after passing through the shock front most of the gas thermalises to a Maxwell-Boltzmann distribution with characteristic post-shock temperature T_2 :

$$f_{\text{th}}(p) = 4\pi n_{\text{th}} \left(\frac{m_p c^2}{2\pi k T_2} \right)^{3/2} p^2 \exp\left(-\frac{m_p c^2 p^2}{2kT_2}\right), \quad (20)$$

where the number density of particles of the thermal distribution in the downstream regime, $n_{\text{th}} = n_2$, as well as T_2 can be inferred by means of the mass, momentum, and energy conservation laws at the shock surface for a gas composed of CRs and thermal constituents. In a companion paper, we describe a formalism for instantaneously and self-consistently inferring the shock strength and all other relevant quantities in the downstream regime of the shock within the framework of SPH simulations (Pfrommer et al. 2006). Assuming that a fraction of the thermalised particles experience stochastic shock acceleration by diffusing back and forth over the shock front, the test particle theory of diffusive shock acceleration predicts a resulting CR power-law distribution in momentum space. Within our model, this CR injection mechanism can be treated as an instantaneous process.

For a particle in the downstream region of the shock to return upstream it is necessary to meet two requirements. The particle's effective velocity component parallel to the shock normal has to be larger than the velocity of the shock wave, and secondly, its energy has to be large enough to escape the "trapping" process by Alfvén that are generated in the downstream turbulence (Malkov & Völk 1995; Malkov & Völk 1998). Thus, only particles of the high-energy tail of the distribution are able to return to the upstream shock regime in order to become accelerated. The complicated detailed physical processes of the specific underlying acceleration mechanism are conveniently compressed into a few parameters (Jones & Kang 1993; Berezhko et al. 1994; Kang & Jones 1995), one of which defines the momentum threshold for the particles of the thermal distribution to be accelerated,

$$q_{\text{inj}} = x_{\text{inj}} p_{\text{th}} = x_{\text{inj}} \sqrt{\frac{2kT_2}{m_p c^2}}. \quad (21)$$

Since Coulomb and ionisation losses efficiently modify the low energy part of the injected CR spectrum, we propose to follow the recipe presented at the end of Sect. 3.1.2, i.e. to simply increase the low energy spectral break of the actually injected spectrum without changing the normalisation of the CR spectrum.

In the linear regime of CR acceleration, the thermal distribution joins in a smooth manner into the resulting CR power-law distribution at q_{inj} so that x_{inj} represents the only parameter in our simplified diffusive shock acceleration model,

$$f_{\text{CR,lin}}(p) = f_{\text{th}}(q_{\text{inj}}) \left(\frac{p}{q_{\text{inj}}} \right)^{-\alpha_{\text{inj}}} \theta(p - q_{\text{inj}}). \quad (22)$$

Fixing the normalisation of the injected CR spectrum by this continuity condition automatically determines C_{inj} which depends on the second adiabatic invariant. The slope of the injected CR spectrum is given by

$$\alpha_{\text{inj}} = \frac{r+2}{r-1}, \quad \text{where } r = \frac{\rho_2}{\rho_1} = \frac{v_1}{v_2} \quad (23)$$

denotes the shock compression ratio (Bell 1978a,b; Drury 1983). In the linear regime, the number density of injected CR particles is given by

$$\Delta n_{\text{CR,lin}} = \int_0^\infty dp f_{\text{CR,lin}}(p) = f_{\text{th}}(q_{\text{inj}}) \frac{q_{\text{inj}}}{\alpha_{\text{inj}} - 1}. \quad (24)$$

This enables us to infer the particle injection efficiency which is a measure of the fraction of downstream thermal gas particles which experience diffusive shock acceleration,

$$\eta_{\text{CR,lin}} \equiv \frac{\Delta n_{\text{CR,lin}}}{n_{\text{th}}} = \frac{4}{\sqrt{\pi}} \frac{x_{\text{inj}}^3}{\alpha_{\text{inj}} - 1} e^{-x_{\text{inj}}^2}. \quad (25)$$

The particle injection efficiency is independent of the downstream post-shock temperature T_2 . These considerations allow us to infer the dynamically relevant injected CR energy density in the linear regime:

$$\Delta \mathcal{E}_{\text{CR,lin}} = \eta_{\text{CR,lin}} T_{\text{CR}}(\alpha_{\text{inj}}, q_{\text{inj}}) n_{\text{th}}(T_2). \quad (26)$$

In our description, the CR energy injection efficiency in the linear regime is defined to be the energy density ratio of freshly injected CRs to the total dissipated energy density in the downstream regime,

$$\zeta_{\text{lin}} = \frac{\Delta \mathcal{E}_{\text{CR,lin}}}{\Delta \mathcal{E}_{\text{diss}}}, \quad \text{where } \Delta \mathcal{E}_{\text{diss}} = \varepsilon_{\text{th}2} - \varepsilon_{\text{th}1} r^\gamma. \quad (27)$$

The dissipated energy density in the downstream regime, $\Delta \mathcal{E}_{\text{diss}}$, is given by the difference of the thermal energy densities in the pre- and post-shock regimes, corrected for the contribution of the adiabatic part of the energy increase due to the compression of the gas over the shock.

In order to obey energy conservation as well as the equations of the linear theory of diffusive shock acceleration, ζ_{lin} has to fulfill a boundary condition which ensures that the dynamical pressure exerted by CRs is smaller than the ram pressure $\rho_1 v_1^2$ of the flow, yielding

$$\frac{P_{\text{CR}}}{\rho_1 v_1^2} = \frac{(\alpha - 1) c^2 \eta_{\text{CR,lin}} q_{\text{inj}}^{\alpha-1} \mathcal{B}_{\frac{1}{1+q_{\text{inj}}^2}} \left(\frac{\alpha-2}{2}, \frac{3-\alpha}{2} \right)}{6 v_1 v_2} < 1, \quad (28)$$

where $\alpha = \alpha_{\text{inj}}$.

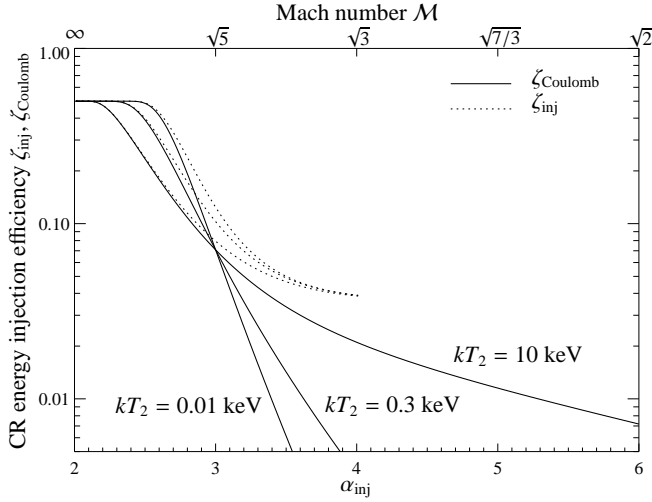


Fig. 3. CR energy injection efficiency for the diffusive shock acceleration process. Shown is the CR energy injection efficiency ζ_{inj} (dotted) for the three post-shock temperatures $kT_2/\text{keV} = 0.01, 0.3,$ and 10 . An effective CR energy efficiency ζ_{Coulomb} (solid) is obtained by considering Coulomb losses which remove the low-energetic part of the injected CR spectrum on a short timescale. In this figure, we adopted the following values for our model parameters, $x_{\text{inj}} = 3.5$, $\zeta_{\text{max}} = 0.5$, and $q_{\text{Coulomb}} = 0.03$.

In typical applications like cosmological SPH simulations, this boundary condition can be substantially simplified. To this end, we propose the following modification of the CR energy injection efficiency in order to account for the saturation effect at high values of the Mach number:

$$\zeta_{\text{inj}} = \left[1 - \exp\left(-\frac{\zeta_{\text{lin}}}{\zeta_{\text{max}}}\right) \right] \zeta_{\text{max}}. \quad (29)$$

Numerical studies of shock acceleration suggest a value of $\zeta_{\text{max}} \approx 0.5$ for the limiting case of the CR energy injection efficiency (Ryu et al. 2003). One can then infer the injected CR energy density in terms of the energy injection efficiency of diffusive shock acceleration processes,

$$\Delta\varepsilon_{\text{CR,inj}} = \zeta_{\text{inj}} \Delta\varepsilon_{\text{diss}}. \quad (30)$$

We note that nonlinear effects, in the form of back-reactions of the accelerated particles upon the shock, change the expectations with respect to the linear case. These effects are expected to be important well before the limit given by Eqn. (29) (see Eichler 1979; Drury & Voelk 1981; Axford et al. 1982; Malkov et al. 2000; Blasi 2002; Blasi et al. 2005; Kang & Jones 2005, and many others).

(DELETED TEXT)

The average kinetic energy of $T_{\text{CR}}(\alpha_{\text{inj}}, q_{\text{inj}})$ of an injection power-law spectrum with CR spectral index α_{inj} is given by Eqn. (34), but with the lower CR momentum cutoff of Eqn. (21). In combination with the slope α_{inj} , the value of x_{inj} regulates the amount of kinetic energy which is transferred to the CRs. Theoretical studies of shock acceleration at galactic supernova remnants suggest a range of $x_{\text{inj}} \approx 3.3$ to 3.6 , implying a particle injection efficiency of $\eta_{\text{CR,lin}} \approx 10^{-4}$ to 10^{-3} (Drury et al. 1989; Jones & Kang 1993; Berezhko et al. 1994; Kang & Jones 1995; Malkov & Völk 1995).

Fig. 3 shows the CR energy injection efficiency ζ_{inj} as a function of spectral index α_{inj} . It can be clearly seen that our simplified model for the diffusive shock acceleration fails in the limit

of weak shocks where it over-predicts the injection efficiency. Especially in this regime, Coulomb and ionisation losses have to be taken into account which remove the low-energetic part of the injected CR spectrum efficiently on a short timescale (cf. Sect. 3.4 & 3.5). This gives rise to an effective CR energy efficiency ζ_{Coulomb} which is obtained by keeping the normalisation of the CR spectrum fixed while simultaneously increasing the cutoff: $q_{\text{inj}} \rightarrow q_{\text{Coulomb}}$.¹ Thus, in the linear regime, the effectively injected CR energy density is given by

$$\Delta\varepsilon_{\text{CR,lin,Coulomb}} = \Delta n_{\text{CR,lin}} T_{\text{CR}}(\alpha_{\text{inj}}, q_{\text{Coulomb}}) \left(\frac{q_{\text{Coulomb}}}{q_{\text{inj}}} \right)^{1-\alpha_{\text{inj}}}. \quad (31)$$

The effective CR energy efficiency ζ_{Coulomb} in the linear regime is obtained by analogy to the previous considerations,

$$\zeta_{\text{lin,Coulomb}} = \frac{\Delta\varepsilon_{\text{CR,lin,Coulomb}}}{\Delta\varepsilon_{\text{diss}}}. \quad (32)$$

Following our suggestion for saturation effects of the shock acceleration given in Eqn. (29), we can obtain the effectively injected CR energy density in the non-linear regime $\Delta\varepsilon_{\text{CR,inj,Coulomb}}$. Assuming a dominant thermal gas component, the spectral index α_{inj} can be translated into the Mach number of the shock, \mathcal{M}_1 , depending on the adiabatic index of the thermal gas γ ,

$$\mathcal{M}_1 = \sqrt{\frac{2(2 + \alpha_{\text{inj}})}{1 + 2\alpha_{\text{inj}} - 3\gamma}}. \quad (33)$$

For a pure thermal gas, the spectral index $\alpha_{\text{inj}} = 2$ formally corresponds to an infinite Mach number. In the case of a varying spectral index, we re-map the changes $\Delta\varepsilon_{\text{CR,inj}}$, $\Delta n_{\text{CR,inj}}$, and the computed value of the injection spectral index $\alpha_{\text{inj}} = (r + 2)/(r - 1)$ onto the dynamical CR variables (C, q, α) which describe the total CR population.

3.1.1. CR injection by structure formation shock waves

For estimating the CR injection at structure formation shock waves in a numerical simulation a dynamical Mach-number finder is required, which identifies and characterises shock waves on the fly. Such a Mach number finder for SPH simulations is presented and tested in Pfrommer et al. (2006), and applied to the problem of CR injection efficiencies of the different shock waves in the large scale structure.

3.1.2. CR injection by supernovae

Shock waves in supernova remnants are believed to be the most important CR injection mechanism in the galactic context. However, for typical simulations of galaxy and structure formation the spatial scales of supernovae are below the resolution length. Therefore we need a sub-grid description for supernova CR injection.

A significant fraction $\zeta_{\text{SN}} \sim 0.1 - 0.3$ of the kinetic energy of a supernova may end up in the CR population. Therefore we set the energy injection rates into the CR and thermal pools to $(d\varepsilon_{\text{CR}}/dt)_{\text{SN}} = \zeta_{\text{SN}} d\varepsilon_{\text{SN}}/dt$ and $(d\varepsilon_{\text{th}}/dt)_{\text{SN}} = (1 - \zeta_{\text{SN}}) d\varepsilon_{\text{SN}}/dt$, respectively. Here $d\varepsilon_{\text{SN}}/dt$ is the total SN energy release rate

¹ Solely for illustration purposes, we sketch how the acceleration efficiency is modified for a constant Coulomb cutoff while we refer to Jubelgas et al. (2006) for an algorithm to compute this cutoff on the fly in simulations.

per volume. The increase in CR number density is given by $(dn_{\text{CR}}/dt)_{\text{SN}} = (d\varepsilon_{\text{CR}}/dt)_{\text{SN}}/T_{\text{CR}}^{\text{inj}}$, where

$$T_{\text{CR}}^{\text{inj}} = m_p c^2 \left[\frac{q_{\text{inj}}^{\alpha_{\text{inj}}-1}}{2} \mathcal{B}_{\frac{1}{1+q^2}} \left(\frac{\alpha-2}{2}, \frac{3-\alpha}{2} \right) + \sqrt{1+q_{\text{inj}}^2} - 1 \right] \quad (34)$$

is the average kinetic energy of an injection power-law spectrum with spectral index α_{inj} and lower momentum cutoff q_{inj} . A plausible value for the injection spectral index is $\alpha_{\text{inj}} = 2.4$ in a galactic context. The low-momentum cutoff can be set to $q_{\text{inj}} \sim \sqrt{kT/(m_p c^2)}$ since the power-law spectrum resulting from shock acceleration reaches down to the thermal population with temperature kT .

However, in numerical practice it may be more economical to use a somewhat higher value for q_{inj} , because in many circumstances Coulomb and ionisation losses will rapidly remove the low energy part of the CR spectrum, so that the energy of these CRs is nearly instantaneously reappearing as thermal energy shortly after injection. A slight re-calibration of ζ_{SN} can take this into account, so that a numerical code does not have to explicitly follow the appearance of a short-lived, low energy, super-thermal CR population.

A criterion to find an adequate q_{inj} is the requirement that the injected CR spectrum above q_{inj} has a cooling time $\tau_{\text{cool}}(q_{\text{inj}}, \alpha_{\text{inj}})$ which equals the energy injection timescale τ_{inj} defined as the ratio of the present CR energy to the energy injection rate (above q_{inj}).² The rationale behind this approach is that injected CRs with $p < q_{\text{inj}}$ would not survive energy losses sufficiently long to make a significant change to the existing CR population given the current injection rate. Further mathematical details about this description can be found in Sec. 4.1.2.

In the case of a varying spectral index, we also have to calculate the pressure injection rate \dot{P}_{CR} for the injection spectrum according to Eq. (6).

3.2. CR diffusion

The ubiquitous cosmic magnetic fields prevent charged relativistic particles to travel macroscopic distances with their intrinsic velocity close to the speed of light. Instead, the particles gyrate around, and travel slowly along magnetic field lines. Occasionally, they get scattered on magnetic irregularities. On macroscopic scales, the transport can often be described as a diffusion process if the gyro-radius can be regarded to be small. The diffusion is highly anisotropic with respect to the direction of the local magnetic field, characterised by a parallel κ_{\parallel} and a perpendicular κ_{\perp} diffusion coefficient. Both are usually functions of location and particle momentum.

Microscopically, the scattering of the CR on magnetic irregularities of MHD waves slows down the parallel transport, but allows the perpendicular transport since it de-places the gyro-centre of the CRs. Therefore, both microscopic diffusion coefficients depend on the scattering frequency ν_{scatt} , but with inverse

proportionalities: $\kappa_{\parallel} \propto \nu_{\text{scatt}}^{-1}$ and $\kappa_{\perp} \propto \nu_{\text{scatt}}$. Particles are best scattered by MHD waves with a wavelength comparable to the CR's gyro-radii, which itself depends on the particle momentum. The various wavelength bands are populated with different strength. Therefore, the scattering frequency is usually a function of the particle momentum. The exact functional dependence is determined by the plasma turbulence spectrum on scales comparable to the CR gyro-radii.

In this picture (e.g. see Bieber & Matthaeus 1997), the diffusion coefficients can be written as

$$\kappa_{\parallel} = \frac{\kappa_{\text{Bohm}}}{\varepsilon} \quad (35)$$

$$\kappa_{\perp} = \frac{\varepsilon}{1 + \varepsilon^2} \kappa_{\text{Bohm}}. \quad (36)$$

Here, $\varepsilon \ll 1$ is the ratio of the scattering frequency ν_{scatt} to the gyro-frequency $\Omega = v/r_g$, and $\kappa_{\text{Bohm}} = v r_g/3 = v p m_p c^2/(3 Z e B)$ is the Bohm diffusion coefficient. In most circumstances, κ_{\perp} will be many orders of magnitude smaller than κ_{\parallel} . Thus, from a microscopic point of view, CR cross field diffusion seems to be nearly impossible.

Macroscopically, the cross-field particle transport is much faster than the microscopic diffusion coefficient suggests. The reason for this is that any small displacement from the initial field line, which a CR achieved by a perpendicular microscopic diffusion step, can be strongly (often exponentially) amplified if the CR travels along its new field line (Rechester & Rosenbluth 1978; Duffy et al. 1995). This is caused by diverging magnetic field lines due to a random walk in a turbulent environment. This effect should always be present at some level even if a large-scale mean field dominates the general magnetic field orientation. The resulting effective diffusion coefficient $\bar{\kappa}_{\perp}$ is difficult to estimate from first principles (see the discussion in Enßlin 2003), but its dependence on the particle momentum is the same as that of the parallel diffusion coefficient, due to the dominant role the parallel diffusion plays in the effective cross field transport. We therefore assume

$$\bar{\kappa}_{\perp}(p) = \delta_{\perp} \kappa_{\parallel}(p) \quad (37)$$

with typically $\delta_{\perp} \sim 10^{-4} - 10^{-2}$ (Giagalone & Jokipii 1999; Enßlin 2003), but see Narayan & Medvedev (2001) for arguments of a larger $\delta_{\perp} \sim 10^{-1}$. In order to be flexible about the underlying MHD turbulence which fixes the momentum dependency of κ_{\parallel} , we assume

$$\bar{\kappa}_{\parallel}(p) = \kappa_{\parallel}(p) = \kappa_0 \beta p^{d_p} \gamma^{d_\gamma} = \kappa_0 p^{d_p+1} \gamma^{d_\gamma-1}. \quad (38)$$

The velocity factor β expresses the reduction of diffusion speed for non-relativistic particles. For a power-law turbulence spectrum of the form $E(k) dk \propto k^{-\alpha_{\text{turb}}} dk$ one obtains $d_p = 2 - \alpha_{\text{turb}}$ and $d_\gamma = 0$, e.g. $d_p = \frac{1}{3}$ for a Kolmogorov-type spectrum. We have included the parameter d_γ in order to allow for low-energy deviations from a pure momentum power-law dependence. Such deviations can for example be caused by modifications of the turbulence spectrum due to MHD-wave-damping by the low-energy bulk of the CR population with small gyro-radii.

It should be noted that turbulent motions in the gas also lead to an effective diffusion (e.g. Cho & Lazarian 2004). Due to the Lagrangian nature of our CR-fluid description, any turbulent diffusion due to numerically resolved eddies is automatically included. Unresolved turbulence, however, may have to be taken separately into account by adding a momentum independent diffusion term to Eqn. (38).

² Another criterion could also be given by the requirement that the Coulomb-loss timescale $\tau_c(q_{\text{inj}}) = |T_p(q_{\text{inj}})/(dT_p(q_{\text{inj}})/dt)_c|$ (see Eqn. (54)) of the particles near the injection cutoff should be on the order of the simulation time-step. However, this approach has two potential shortcomings: First, the dynamics becomes formally time-step dependent, although the Coulomb cooling dynamics will largely compensate for this. Second, if small numerical timesteps permit $q_{\text{inj}} \ll q \sim 1$, the large number of low energy CRs injected may drag an existing CR population to lower energies, due to our simplified CR dynamics.

The equation describing the evolution of the CR spectrum $f(\mathbf{x}, p, t)$ due to diffusion is

$$\left(\frac{\partial f}{\partial t}\right)_{\text{diff}} = \frac{\partial}{\partial x_i} \kappa_{ij} \frac{\partial f}{\partial x_j}, \quad (39)$$

where the diffusion tensor

$$\kappa_{ij}(p) = \kappa_{\parallel}(p) [b_i b_j + \delta_{\perp} (\delta_{ij} - b_i b_j)] = \tilde{\kappa}_{ij} p^{d_p+1} \gamma^{d_\gamma-1} \quad (40)$$

is anisotropic with respect to the local main magnetic field direction $\mathbf{b}(\mathbf{x}) = \mathbf{B}(\mathbf{x})/B(\mathbf{x})$. Since we are interested in a simplified description, we have to translate Eqn. (39) into changes of CR number and energy density. Integrating Eqn. (39) over p leads to an equation governing the change in CR number density due to diffusion:

$$\left(\frac{\partial n_{\text{CR}}}{\partial t}\right)_{\text{diff}} = \frac{\partial}{\partial x_i} \tilde{\kappa}_{ij} \frac{\partial}{\partial x_j} \left\{ \frac{C}{\alpha - 2 - d_p} \left[q^{-\alpha+2+d_p} (1+q^2)^{-\frac{1-d_\gamma}{2}} - \frac{1-d_\gamma}{2} \mathcal{B}_{\frac{1}{1+q^2}} \left(\frac{\alpha-1-d_p-d_\gamma}{2}, \frac{4+d_p-\alpha}{2} \right) \right] \right\}. \quad (41)$$

This can only lead to reasonable results if the condition $\alpha > 1 + d_p + d_\gamma$ is fulfilled. For a Kolmogorov-turbulence diffusion coefficient ($d_p = \frac{1}{3}$, $d_\gamma = 0$), this translates into $\alpha > 1.33$.

One could assume that the transported energy is simply $(d\mathcal{E}_{\text{CR}})_{\text{diff}} = T_{\text{CR}} (dn_{\text{CR}})_{\text{diff}}$. However, this ansatz would ignore that the more energetic particles diffuse faster, implying that the effective CR energy diffusion is more rapid than the CR number diffusion. In order to model this, we multiply Eqn. (39) by $T_p(p)$ and integrate over p . This leads to

$$\left(\frac{\partial \mathcal{E}_{\text{CR}}}{\partial t}\right)_{\text{diff}} = \frac{\partial}{\partial x_i} \tilde{\kappa}_{ij} \frac{\partial}{\partial x_j} \left\{ \frac{C m_p c^2}{\alpha - 2 - d_p} \times \left[q^{-\alpha+2+d_p} \left((1+q^2)^{\frac{d_\gamma}{2}} - (1+q^2)^{\frac{d_\gamma-1}{2}} \right) + \frac{1-d_\gamma}{2} \mathcal{B}_{\frac{1}{1+q^2}} \left(\frac{\alpha-1-d_p-d_\gamma}{2}, \frac{4+d_p-\alpha}{2} \right) + \frac{d_\gamma}{2} \mathcal{B}_{\frac{1}{1+q^2}} \left(\frac{\alpha-2-d_p-d_\gamma}{2}, \frac{4+d_p-\alpha}{2} \right) \right] \right\}. \quad (42)$$

This equation can only give reasonable results if the condition $\alpha > 2 + d_p + d_\gamma$ is fulfilled. For a Kolmogorov-turbulence diffusion coefficient ($d_p = \frac{1}{3}$, $d_\gamma = 0$), this translates into $\alpha > 2.33$.

In the case of a varying spectral index, we need to compute $(\partial P_{\text{CR}}/\partial t)_{\text{diff}}$ which can be obtained by multiplying Eqn. (39) by $p\beta(p)$ and integrating over p . This results in

$$\left(\frac{\partial P_{\text{CR}}}{\partial t}\right)_{\text{diff}} = \frac{\partial}{\partial x_i} \tilde{\kappa}_{ij} \frac{\partial}{\partial x_j} \frac{C m_p c^2}{6} \times \mathcal{B}_{\frac{1}{1+q^2}} \left(\frac{\alpha-2-d_p-d_\gamma}{2}, \frac{4+d_p-\alpha}{2} \right). \quad (43)$$

This equation can only lead to reasonable results if again the condition $\alpha > 2 + d_p + d_\gamma$ is fulfilled.

3.3. CR in-situ re-acceleration

The diffusive propagation of CRs implies that CR particles scatter resonantly on plasma waves with wavelength comparable to their gyro-radii. Since these waves are propagating, the CRs exchange not only momentum, but also energy with the waves,

leading to a re-acceleration of an existing cosmic ray population. Since the CR-number is not changed by this process, we can state:

$$\left(\frac{\partial n_{\text{CR}}}{\partial t}\right)_{\text{re-acc}} = 0. \quad (44)$$

The change in the CR energy can be derived from the Fokker-Planck equation for the 3-dimensional momentum distribution function $f^{(3)}(p) = f(p)/(4\pi p^2)$ of an isotropic CR distribution:

$$\left(\frac{\partial f^{(3)}(p)}{\partial t}\right)_{\text{re-acc}} = \frac{1}{p^2} \frac{\partial}{\partial p} \left(p^2 D_p \frac{\partial f^{(3)}}{\partial p} \right), \quad (45)$$

where D_p is the (pitch-angle averaged) momentum-space diffusion coefficient. D_p is a function of p , which we parametrise by

$$D_p = D_0 p^{1-a_p} \gamma^{1-a_\gamma}. \quad (46)$$

We note that here, as in the section on CR diffusion, a power-law spectrum of the relevant plasma waves is assumed, as it is expected in the inertial range of MHD turbulence. In case the CRs are numerous enough to extract energy from the wave spectrum with a considerable rate (compared to the wave-cascade or -decay time of the turbulence), the wave spectrum itself would be modified, reducing the acceleration efficiency. A self-consistent description would therefore also need to follow the wave spectrum and its modification due to the energy extraction by CRs (e.g. Miller et al. 1996; Brunetti et al. 2004; Ptuskin et al. 2005; Brunetti & Lazarian 2007). However, this is beyond the scope of this paper. Thus, as soon the cosmic ray population becomes important due to re-acceleration, our description has probably left its range of validity.

Taking the appropriate moments of Eqn. (45) leads to evolution equations for the CR number density, Eqn. (44), and for the CR energy density,

$$\left(\frac{\partial \mathcal{E}_{\text{CR}}}{\partial t}\right)_{\text{re-acc}} = (2+\alpha) C D_0 m_p c^2 \times \left[\frac{1}{2} \mathcal{B}_{\frac{1}{1+q^2}} \left(\frac{\alpha+a_p+a_\gamma-2}{2}, \frac{2-\alpha-a_p}{2} \right) + \left(\sqrt{1+q^2} - 1 \right) q^{\alpha-a_p} (1+q^2)^{(1-a_\gamma)/2} \right], \quad (47)$$

which is valid for $\alpha > 2 - a_p - a_\gamma$. This energy has to be taken from the kinetic-energy dissipation budget of the hydrodynamical flow. In the case of a varying spectral index, we can obtain the evolution equation for the CR pressure by taking the appropriate moment of Eqn. (45),

$$\left(\frac{\partial P_{\text{CR}}}{\partial t}\right)_{\text{re-acc}} = (2+\alpha) C D_0 \frac{m_p c^2}{3} \times \left[\mathcal{B}_{\frac{1}{1+q^2}} \left(\frac{\alpha+a_p+a_\gamma}{2}, \frac{2-\alpha-a_p}{2} \right) + \frac{1}{2} \mathcal{B}_{\frac{1}{1+q^2}} \left(\frac{\alpha+a_p+a_\gamma-2}{2}, \frac{4-\alpha-a_p}{2} \right) + q^{2-\alpha-a_p} (1+q^2)^{-a_\gamma/2} \right], \quad (48)$$

which is valid for $\alpha > 2 - a_p - a_\gamma$.

The parameterisation of the momentum diffusion coefficient is chosen to be similar to the one for the spatial diffusion coefficient because of their related physical background: both are

due to scattering on the same plasma waves. Quasi-linear calculations of the Fokker-Planck transport coefficient of charged particles interacting with plasma waves (see Schlickeiser 2002) demonstrate that both, the spatial- and the momentum-diffusion coefficient depend mainly on the pitch-angle diffusion coefficient $D_{\mu\mu} = D_{\mu\mu}(p, \mu)$, where $\mu = \cos\theta$ is the cosine of the pitch-angle θ :

$$D_p = \frac{p^2 V_A^2}{v^2} \int_{-1}^1 d\mu D_{\mu\mu}(p, \mu) \quad (49)$$

$$\kappa_{\parallel} = \frac{v^2}{8} \int_{-1}^1 d\mu \frac{(1 - \mu^2)^2}{D_{\mu\mu}(p, \mu)}. \quad (50)$$

Here, V_A is the phase-velocity of the scattering plasma waves which are usually assumed to be Alfvén waves³ with $V_A = B/\sqrt{4\pi\rho}$. In the relevant inertia ranges of the MHD-turbulence spectra, it is expected that the amplitude but not the composition of waves changes with wavelength.⁴ Therefore, the pitch-angle diffusion coefficient should be separable in p and μ , e.g. $D_{\mu\mu}(p, \mu) = D_1(p) D_2(\mu)$. This allows us to relate the two diffusion coefficients via

$$D_p \kappa_{\parallel} = p^2 V_A^2 X_2, \quad (51)$$

where X_2 is a constant of order unity, and is formally given by

$$X_2 = \frac{1}{8} \left(\int_{-1}^1 d\mu D_2(\mu) \right) \left(\int_{-1}^1 d\mu \frac{(1 - \mu^2)^2}{D_2(\mu)} \right). \quad (52)$$

Therefore, in the framework of a quasi-linear approximation, the parameters describing in-situ re-acceleration and diffusion are related by

$$a_p = d_p, \quad a_\gamma = d_\gamma, \quad \text{and} \quad D_0 = V_A^2 X_2 / \kappa_0, \quad (53)$$

e.g. for a Kolmogorov-like spectrum of Alfvén waves $a_p = d_p = \frac{1}{3}$, $a_\gamma = d_\gamma = 0$, and $X_2 \sim O(1)$.

3.4. Coulomb losses

The energy loss of a proton with $\gamma \ll m_p/m_e$ by Coulomb losses in a plasma is given by Gould (1972):

$$-\left(\frac{dT_p(p)}{dt}\right)_C = \frac{4\pi e^4 n_e}{m_e \beta c} \left[\ln\left(\frac{2m_e c^2 \beta p}{\hbar \omega_{pl}}\right) - \frac{\beta^2}{2} \right]. \quad (54)$$

Here, $\omega_{pl} = \sqrt{4\pi e^2 n_e / m_e}$ is the plasma frequency, and n_e is the number density of free electrons. We note that in a neutral gas the Coulomb losses can coarsely be estimated with the same formulae, provided n_e is taken to be the total electron number density (free plus bound). However, atomic charge shielding effects lower the Coulomb losses significantly. A more accurate description of ionisation losses is given in Sect. 3.5.

In order to obtain the Coulomb energy losses of the CR population, one has to integrate Eqn. (54) over the spectrum

³ Also the stronger damped fast magneto-sonic waves are discussed as efficient accelerators due to their higher phase velocity (e.g. Eilek 1979; Cassano & Brunetti 2005).

⁴ This wont be the case anymore as soon some part of the CR population extract a significant amount of the wave-energy budget from the spectral range they can resonate with. In this case the CR and wave spectra become interdependent and a decomposition of the pitch-angle diffusion coefficient into a momentum and a pitch-angle dependent function is impossible (e.g. Miller et al. 1996; Brunetti et al. 2004; Puskun et al. 2005).

$f(p)$. This integration can certainly be performed numerically. For fast and efficient applications, an approximative analytical expression might be more practical. We derive such an expression by replacing the term βp in the Coulomb logarithm with its mean value for the given spectrum, which can be written as $\langle \beta p \rangle = 3 P_{CR} / (m_p c^2 n_{CR})$.⁵ The Coulomb energy losses are then

$$-\left(\frac{d\varepsilon_{CR}}{dt}\right)_C \approx \frac{2\pi C e^4 n_e}{m_e c} \left[\ln\left(\frac{2m_e c^2 \langle \beta p \rangle}{\hbar \omega_{pl}}\right) \mathcal{B}_{\frac{1}{1+q^2}}\left(\frac{\alpha-1}{2}, -\frac{\alpha}{2}\right) - \frac{1}{2} \mathcal{B}_{\frac{1}{1+q^2}}\left(\frac{\alpha-1}{2}, -\frac{\alpha-2}{2}\right) \right] \quad (55)$$

Since Coulomb losses only affect the lower energy part of the spectrum and therefore should leave the normalisation unaffected, we propose to set $(dn_{CR}/dt)_C = (d\varepsilon_{CR}/dt)_C / T_p(q)$. This mimics the effect of Coulomb losses on a spectrum quiet well, since Coulomb losses remove the lowest energy particles most efficiently from the spectrum, moving them into the thermal pool. Because also their energy is thermalised, we have $(d\varepsilon_{th}/dt)_C = -(d\varepsilon_{CR}/dt)_C$ and $(dn_p/dt)_C = -(dn_{CR}/dt)_C$. The second equation (which expresses proton number conservation) can be neglected for convenience due to the smallness of the effect. The case of a varying spectral index can be treated in the same way as for a constant spectral index because Coulomb losses do not significantly modify the spectral index of the ultra-relativistic CR population.

The Coulomb loss time scales $\tau = \varepsilon_{CR} / (d\varepsilon_{CR}/dt)_C$ of CR populations are shown in 4.

3.5. Ionisation losses

Ionisation losses of a proton can be calculated with the Bethe-Bloch equation (Groom & Klein 2000), which we cast into the form

$$-\left(\frac{dT_p(p)}{dt}\right)_I = \frac{4\pi e^4}{m_e \beta c} \sum_Z Z n_Z \left[\ln\left(\frac{2m_e c^2 p^2}{I_Z b(\gamma)}\right) - \beta^2 - \frac{\delta_Z}{2} \right]. \quad (56)$$

Here, n_Z is the number density of atomic species with electron number Z , and I_Z its ionisation potential. $b(\gamma) = \sqrt{1 + 2\gamma m_e / m_p + (m_e / m_p)^2}$ is a minor correction factor for the here relevant regime $\gamma \ll m_p / m_e$, which we ignore in the following. The density correction factor δ_Z is usually not significant for gases, but should be given here for completeness:

$$\delta_Z = \begin{cases} 2y - D_Z & y_{1,Z} < y \\ 2y - D_Z + a_Z((y_{1,Z} - y) / \ln 10)^{k_Z} & y_{0,Z} < y < y_{1,Z} \\ 0 & y < y_{0,Z} \end{cases} \quad (57)$$

Here, $y = \ln p$, $D_z = 1 - 2 \ln(\hbar \omega_{pl} / I_Z)$ and $y_{0,Z}$, $y_{1,Z}$, a_Z , k_Z are empirical constants, which characterise the atomic species (Sternheimer 1952). The values for Hydrogen and Helium can be found in Table 1. It is apparent that the density effect can be neglected below 60 GeV, and therefore we propose to ignore it in applications in which the CR spectrum is trans-relativistic.

Note that the high energy limit of Eq. (56) is similar, but not exactly identical to the Coulomb loss formula Eq. (54).

⁵ This leads to a slight overestimate of the energy losses. A slight underestimate results by setting $\langle \beta p \rangle \rightarrow q^2 / \sqrt{1 + q^2}$ in Eqn. 55. As long these two terms lead to similar loss rates our approximately treatment is a good description. Otherwise the integration has to be performed numerically.

| Element | Z | I_Z | $y_{0,Z}$ | $y_{1,Z}$ | a_Z | k_Z |
|----------------|---|---------|---------------|------------|-------|-------|
| H ₂ | 1 | 13.6 eV | $1.76 \ln 10$ | $3 \ln 10$ | 0.34 | 5.01 |
| He | 2 | 24.6 eV | $2.0 \ln 10$ | $3 \ln 10$ | 0.98 | 4.11 |

Table 1. Atomic parameters as given by Sternheimer (1952). The Hydrogen measurements were done with molecular hydrogen, but no significant changes for atomic hydrogen are expected with the accuracy required for our description.

Similar to the case of the Coulomb losses, we insert characteristic momenta into the logarithmic factors in order to allow for an analytical integration of the energy losses over the CR spectrum. Since the losses are dominated by the trans-relativistic regime, we propose to use simply $\langle p^2 \rangle \approx \langle \beta p \rangle = 3 P_{\text{CR}}/(m_p c^2 n_{\text{CR}})$ and to set $y = \frac{1}{2} \ln \langle p^2 \rangle$ in order to estimate δ_Z . This yields

$$-\left(\frac{d\epsilon_{\text{CR}}}{dt}\right)_I \approx \frac{2\pi C e^4}{m_e c} \sum_Z Z n_Z \left\{ \ln \left(\frac{2m_e c^2 \langle p^2 \rangle}{I_Z} \right) - \frac{\delta_Z}{2} \right\} \times \mathcal{B}_{1+q^2} \left(\frac{\alpha-1}{2}, -\frac{\alpha}{2} \right) - \mathcal{B}_{1+q^2} \left(\frac{\alpha-1}{2}, -\frac{\alpha-2}{2} \right) \quad (58)$$

A by-product of the energy losses is the generation of free electrons. The production rate of free electrons in a Hydrogen gas can be estimated using the empirical observation that per 36 eV lost by the proton on average a free electron is produced, either as a direct or as a secondary knock-on electron (Longair 1992). Therefore, the ionisation rate is

$$\left(\frac{dn_e}{dt}\right)_I \approx -\frac{1}{36 \text{ eV}} \left(\frac{d\epsilon_{\text{CR}}}{dt}\right)_I. \quad (59)$$

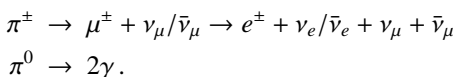
The remaining fraction ($1 - I_1/36\text{eV} = 62\%$) of the energy loss is heating the medium directly. This electron production term can be included in any ionisation equilibrium calculation for the medium.

3.6. Bremsstrahlung losses

Bremsstrahlung energy losses of protons are usually negligible, since they are suppressed by a factor $m_e^2/m_p^2 \approx 3 \cdot 10^{-7}$ compared with electron bremsstrahlung losses, which are in turn usually already small. Therefore, we do not include bremsstrahlung energy losses of protons in our description.

3.7. Hadronic losses

Another important process is the inelastic reaction of CR nuclei with atoms and molecules of interstellar and intergalactic matter. The CR protons interact hadronically with the ambient thermal gas and produce mainly neutral and charged pions, provided their momentum exceeds the kinematic threshold $q_{\text{thr}} m_p c^2 = 0.78 \text{ GeV}$ for the reaction. The neutral pions decay after a mean lifetime of $9 \times 10^{-17} \text{ s}$ into γ -rays while the charged pions decay into secondary electrons (and neutrinos):



With hadronic interactions, only the CR population above the kinematic threshold q_{thr} is visible through its decay products in γ -rays and synchrotron emission. Because of baryon number conservation in strong and electro-weak interactions, we always

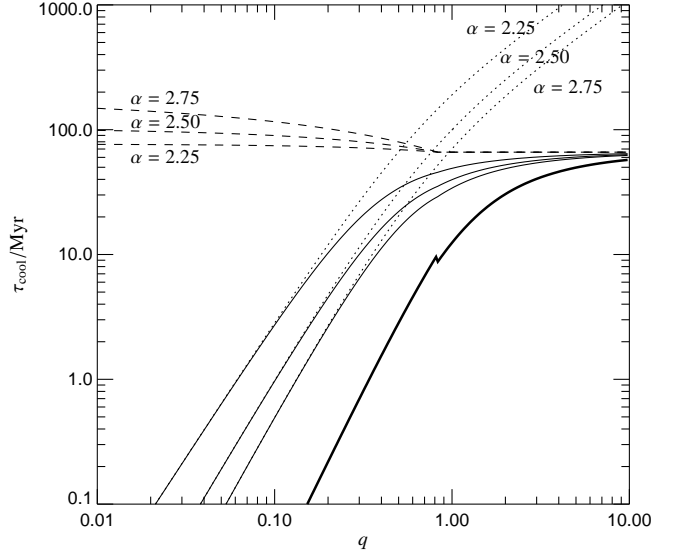


Fig. 4. Cooling times of CR spectra with spectral indices $\alpha = 2.25, 2.50,$ and 2.75 as a function of the cutoff q (thin solid lines) in a pure hydrogen plasma with $n_e = 1 \text{ cm}^{-3}$. Coulomb and hadronic energy loss times are also displayed with dotted and dashed lines, respectively. The thick solid lines gives the total cooling time of a mono-energetic CR population with $p = q$. The feature at $q = 0.83$ is due to the onset of the hadronic losses above this momentum.

end up with pions and two protons in this CR-proton hadronic interaction (the possibly produced neutron will decay after a mean lifetime of 886 s into a second proton). Thus, the CR number density is conserved, implying $(dn_{\text{CR}}/dt)_{\text{had}} = 0$.

The total energy loss of CRs is independent of the detailed mechanisms of how the energy has been imparted on pions during hadronic interactions and given by

$$-\left(\frac{dE_p}{dt}\right)_{\text{had}} = cn_N \sigma_{pp} K_p T_p \theta(p_p - q_{\text{thr}}). \quad (60)$$

Here, σ_{pp} is the total pion cross section which is given by Eqn. (64), $K_p \approx 1/2$ denotes the inelasticity of the reaction in the limiting regime (Mannheim & Schlickeiser 1994), and $n_N = n_e/(1 - \frac{1}{2}X_{\text{He}})$ denotes the target nucleon density in the ICM, assuming primordial element composition with $X_{\text{He}} = 0.24$. The change in energy density of CRs because of hadronic losses is given by

$$\begin{aligned} -\left(\frac{d\epsilon_{\text{CR}}}{dt}\right)_{\text{had}} &= \int_0^\infty dp f(p) \left(\frac{dE_p}{dt}\right)_{\text{had}} \\ &= cn_N \bar{\sigma}_{pp} K_p \epsilon_{\text{CR}} (\max(q, q_{\text{thr}})), \end{aligned} \quad (61)$$

where ϵ_{CR} is given by Eqn. (4) in which the lower spectral break q has to be replaced by $\max(q, q_{\text{thr}})$. The case of a varying spectral index can be dealt with in the same way as a constant spectral index because hadronic losses do not significantly modify the CR spectral index. The hadronic loss time scales $\tau = \epsilon_{\text{CR}}/(\dot{\epsilon}_{\text{CR}})_{\text{had}}$ of CR populations are shown in 4.

3.8. Gamma ray emission

An analytic formula describing the omnidirectional differential γ -ray source function resulting from pion-decay of a power-law CR population is given in Pfrommer & Enßlin (2004), yielding

in our notation:

$$s_\gamma(E_\gamma) dE_\gamma dV \simeq \frac{2^4 C}{3\alpha} \frac{\sigma_{pp} n_N}{m_p c} \left(\frac{m_p}{2m_{\pi^0}} \right)^\alpha \times \left[\left(\frac{2E_\gamma}{m_{\pi^0} c^2} \right)^\delta + \left(\frac{2E_\gamma}{m_{\pi^0} c^2} \right)^{-\delta} \right]^{-\alpha/\delta} dE_\gamma dV. \quad (62)$$

The formalism also includes the detailed physical processes at the threshold of pion production like the velocity distribution of CRs, momentum dependent inelastic CR-proton cross section, and kaon decay channels. The shape parameter δ and the effective cross section σ_{pp} depend on the spectral index of the γ -ray spectrum α according to

$$\delta \simeq 0.14 \alpha^{-1.6} + 0.44 \quad \text{and} \quad (63)$$

$$\sigma_{pp} \simeq 32 \cdot (0.96 + e^{4.4-2.4\alpha}) \text{ mbarn}. \quad (64)$$

There is a detailed discussion in Pfrommer & Enßlin (2004) how the γ -ray spectral index α_γ relates to the spectral index of the parent CR population α . In Dermer's model, the pion multiplicity is independent of energy yielding the relation $\alpha_\gamma = \alpha$ (Dermer 1986a,b).

The derivation of the pion-decay induced γ -ray source function implicitly assumed the kinematic threshold q_{thr} to be above the lower break of the CR spectrum q . This assumption is satisfied in the case of our Galaxy, where a flattening of the CR spectrum occurs below the kinematic energy threshold $E_{\text{thr}} = 1.22 \text{ GeV}$ (Simpson 1983). If the inequality $q < q_{\text{thr}}$ is violated in the simulation for sufficiently long timescales, the resulting γ -ray emission maps have to be treated with caution.

Provided the CR population has a power-law spectrum, the integrated γ -ray source density λ_γ for pion decay induced γ -rays can be obtained by integrating the γ -ray source function $s_\gamma(E_\gamma)$ in Eqn. (62) over an energy interval yielding

$$\lambda_\gamma = \lambda_\gamma(E_1, E_2) = \int_{E_1}^{E_2} dE_\gamma s_\gamma(E_\gamma) \quad (65)$$

$$= \frac{4 C}{3 \alpha \delta} \frac{m_{\pi^0} c \sigma_{pp} n_N}{m_p} \left(\frac{m_p}{2m_{\pi^0}} \right)^\alpha \left[\mathcal{B}_x \left(\frac{\alpha+1}{2\delta}, \frac{\alpha-1}{2\delta} \right) \right]_{x_1}^{x_2}, \quad (66)$$

$$x_i = \left[1 + \left(\frac{m_{\pi^0} c^2}{2E_i} \right)^{2\delta} \right]^{-1} \quad \text{for } i \in \{1, 2\}. \quad (67)$$

3.9. Hadronically induced synchrotron emission

This section describes the hadronically induced radio synchrotron emission while employing the steady-state approximation for the CR electron spectrum following Dolag & Enßlin (2000) and Pfrommer & Enßlin (2004). This is only justified if the dynamical and diffusive timescales are long compared to the synchrotron timescale. This may well be the case in clusters of galaxies, however, probably not in our own Galaxy. Possible re-acceleration processes of CR electrons like continuous in-situ acceleration via resonant pitch angle scattering by turbulent Alfvén waves as well as CR electron injection by other processes are neglected in this approach.

Assuming that the parent CR proton population is represented by the power-law of Eqn. (1), the CR electron population above a GeV is therefore described by a power-law spectrum

$$f_e(E_e) = \frac{C_e}{\text{GeV}} \left(\frac{E_e}{\text{GeV}} \right)^{-\alpha_e}, \quad (68)$$

$$\text{and } C_e = \frac{16^{2-\alpha_e} \sigma_{pp} m_e^2 c^4}{\alpha_e - 2} \frac{n_N C}{\sigma_T \text{ GeV}} \frac{n_N C}{\varepsilon_B + \varepsilon_{\text{ph}}} \left(\frac{m_p c^2}{\text{GeV}} \right)^{\alpha-1}, \quad (69)$$

where the effective CR-proton cross section σ_{pp} is given by Eqn. (64), σ_T is the Thomson cross section, $\varepsilon_B = B^2/(8\pi)$ is the local magnetic field energy density, and $\varepsilon_{\text{ph}} = \varepsilon_{\text{CMB}} + \varepsilon_{\text{stars}}$ is the energy density of the cosmic microwave background (CMB) and starlight photon field. $\varepsilon_{\text{CMB}} = B_{\text{CMB}}^2/(8\pi)$ can be expressed by an equivalent field strength $B_{\text{CMB}} = 3.24 (1+z)^2 \mu\text{G}$. $\varepsilon_{\text{stars}}$ either has to be guessed or calculated from information of the star distribution, or ignored.

The synchrotron emissivity j_ν at frequency ν and per steradian of such a CR electron population (68), which is located in an isotropic distribution of magnetic fields (Eqn. (6.36) in Rybicki & Lightman 1979), is obtained after averaging over an isotropic distribution of electron pitch angles, yielding

$$j_\nu = A_{E_{\text{syn}}}(\alpha_e) C_e \left[\frac{\varepsilon_B}{\varepsilon_{B_c}} \right]^{(\alpha_e+1)/2} \propto \varepsilon_{\text{CRe}} B^{\alpha_e+1} \nu^{-\alpha_e}, \quad (70)$$

$$B_c = \sqrt{8\pi \varepsilon_{B_c}} = \frac{2\pi m_e^3 c^5 \nu}{3 e \text{ GeV}^2} \simeq 31 \left(\frac{\nu}{\text{GHz}} \right) \mu\text{G}, \quad (71)$$

$$A_{E_{\text{syn}}} = \frac{\sqrt{3\pi} B_c e^3}{32\pi m_e c^2} \frac{\alpha_e + \frac{7}{3} \Gamma\left(\frac{3\alpha_e-1}{12}\right) \Gamma\left(\frac{3\alpha_e+7}{12}\right) \Gamma\left(\frac{\alpha_e+5}{4}\right)}{\alpha_e + 1 \Gamma\left(\frac{\alpha_e+7}{4}\right)}, \quad (72)$$

where $\Gamma(a)$ denotes the Γ -function (Abramowitz & Stegun 1965), $\alpha_\nu = (\alpha_e - 1)/2 = \alpha/2$, and B_c denotes a (frequency dependent) characteristic magnetic field strength which implies a characteristic magnetic energy density ε_{B_c} .

4. Testing the accuracy of the formalism

The rigid spectral form of a single power-law with cutoff, which is imposed on the CR populations in our formalism, leads to inaccuracies compared to the proper spectral solutions of the evolution equations of the CR spectra. The question is how large are the inaccuracies for different physical quantities, and under which circumstances they can or cannot be tolerated.

Two tests are presented: a steady state situation, where cooling balances injection and a time dependent, freely cooling CR spectrum, without injection.

4.1. Steady state CR spectrum

4.1.1. Accurate steady state spectrum

In order to address these questions we analyse a steady state situation in which accurate and approximated spectra can be worked out analytically. In a homogeneous environment the CR spectrum $f(p, t)$ should follow the evolution equation

$$\frac{\partial f(p, t)}{\partial t} + \frac{\partial}{\partial p} (\dot{p}(p) f(p, t)) = Q(p) - \frac{f(p, t)}{\tau_{\text{loss}}(p)}, \quad (73)$$

where

$$\dot{p}(p) = \left[\left(\frac{dT_p(p)}{dt} \right)_C + \left(\frac{dT_p(p)}{dt} \right)_{\text{cata}} \right] \left(\frac{dT_p(p)}{dp} \right)^{-1} \quad (74)$$

is the momentum loss rate due to Coulomb- and hadronic losses⁶ (see Eqs. (54) & (60)). We assume a fully ionized Hydrogen plasma with a thermal electron density of $n_e = 1 \text{ cm}^{-3}$. A time-independent CR injection spectrum

$$Q(p) = Q_{\text{inj}} p^{-\alpha_{\text{inj}}}, \quad (75)$$

⁶ We approximate here the hadronic losses as a continuous energy loss.

with an injection normalisation $Q_{\text{inj}} = 1 \text{ Myr}^{-1}$ (for a here unspecified volume element) and $\alpha_{\text{inj}} = 2.5$ is assumed. The environment is assumed to be sufficiently extended so that particle escape can be ignored, implying $\tau_{\text{loss}}(p) = \infty$ except for the thermalisation of CRs at very low momenta.

The steady state spectrum is then given by

$$f(p) = \frac{Q_{\text{inj}} p^{1-\alpha_{\text{inj}}}}{|\dot{p}(p)|(\alpha_{\text{inj}} - 1)} \approx \frac{Q_{\text{inj}} p^{-\alpha_{\text{inj}}}}{(\alpha_{\text{inj}} - 1)A_{\text{C}}} \begin{cases} p^3 & : p \ll p_* \\ p^3 & : p \gg p_* \end{cases}, \quad (76)$$

and its energy distribution can be seen in Fig. 5. The asymptotic approximations assume negligible hadronic and Coulomb losses in the low and high energy regimes, respectively. Furthermore, the weak logarithmic dependence of the Coulomb losses on the particle momentum was ignored in the asymptotic equations. The cross-over momentum $p_* \approx 1$ depends on the ratio of the Coulomb to hadronic loss rates coefficients

$$A_{\text{C}} = \frac{4\pi e^4 n_e}{m_e c} \ln\left(\frac{2m_e c^2 \beta p}{\hbar\omega_{\text{pl}}}\right) \quad (77)$$

$$A_{\text{had}} = \sigma_{\text{pp}} K_{\text{p}} m_{\text{p}} c^3 n_{\text{N}} \quad (78)$$

and is given by

$$p_* = \sqrt[3]{\frac{A_{\text{C}}}{A_{\text{had}}}} = \sqrt[3]{\frac{4\pi e^4 n_e \ln((2m_e c^2)/(\hbar\omega_{\text{pl}}))}{m_e m_{\text{p}} c^4 \sigma_{\text{pp}} K_{\text{p}} n_{\text{N}}}} \approx 1.087. \quad (79)$$

Here, we have inserted a fiducial electron density of $n_e = 1 \text{ cm}^{-3}$ and assumed a pure hydrogen plasma. $p_* \approx 1.1$ is accurate to 10% for electron densities in the range $[10^{-6}, 10^3] \text{ cm}^{-3}$. As a reference case for an analytic approximation to the steady state equilibrium CR spectrum we introduce a simple matched asymptotic solution:

$$f_{\text{approx}}(p) \approx \frac{Q_{\text{inj}} p^{-\alpha_{\text{inj}}}}{(\alpha_{\text{inj}} - 1)A_{\text{C}}(p_*^{-3} + p^{-3})}, \quad (80)$$

which is also displayed in Fig. 5.

4.1.2. Approximate steady state spectrum

In this section, we calculate the equilibrium spectrum provided by our simplified CR formalism. Since our formalism is based on CR particle and energy conservation, the injected particle number and energy should balance the ones due to Coulomb and hadronic losses. CR energy balance therefore yields $d\mathcal{E}_{\text{CR}}/dt = (d\mathcal{E}_{\text{CR}}/dt)_{\text{inj}} + (d\mathcal{E}_{\text{CR}}/dt)_{\text{cool}} = 0$ which is equivalent to

$$\left(\frac{d\mathcal{E}_{\text{CR}}}{dt}(Q_{\text{inj}}, q_{\text{inj}}, \alpha_{\text{inj}})\right)_{\text{inj}} = \frac{\mathcal{E}_{\text{CR}}(C, q, \alpha)}{\tau_{\text{cool}}(q, \alpha)} \quad (81)$$

The CR cooling time-scale due to Coulomb and hadronic losses is defined by

$$\tau_{\text{cool}}^{-1}(q, \alpha) = \tau_{\text{C}}^{-1}(q, \alpha) + \tau_{\text{had}}^{-1}(q, \alpha) = \frac{\left(\frac{d\mathcal{E}_{\text{CR}}}{dt}(C, q, \alpha)\right)_{\text{C+had}}}{\mathcal{E}_{\text{CR}}(C, q, \alpha)}. \quad (82)$$

The injected number of particles must be balanced by the number of particles removed from the CR population due to Coulomb losses, since hadronic losses conserve particle number in the spectrum: $dn_{\text{CR}}/dt = (dn_{\text{CR}}/dt)_{\text{inj}} + (dn_{\text{CR}}/dt)_{\text{C}} = 0$. Since $(dn_{\text{CR}}/dt)_{\text{C}} = (d\mathcal{E}_{\text{CR}}/dt)_{\text{C}}/T_{\text{p}}(p)$ we get

$$\left(\frac{dn_{\text{CR}}}{dt}(Q_{\text{inj}}, q_{\text{inj}}, \alpha_{\text{inj}})\right)_{\text{inj}} = \frac{\mathcal{E}_{\text{CR}}(C, q, \alpha)}{T_{\text{p}}(q) \tau_{\text{C}}(q, \alpha)}. \quad (83)$$

Dividing Eq. (81) by Eq. (83) yields

$$T_{\text{CR}}(q_{\text{inj}}, \alpha_{\text{inj}}) = T_{\text{p}}(q) \left(1 + \frac{\tau_{\text{C}}(q, \alpha)}{\tau_{\text{had}}(q, \alpha)}\right), \quad (84)$$

which is free of any normalisation constant (C, C_{inj}) and defines an implicit function relating the injection cutoff q_{inj} and the equilibrium cutoff $q = q(q_{\text{inj}}, \alpha_{\text{inj}}, \alpha)$.

In order to specify q fully a second condition between q and q_{inj} is required. A very simplistic, but – as we will see a posteriori – sometimes reasonable choice, is the condition $q_{\text{inj}} = q$. However, our criterion to specify q_{inj} is the requirement that the injected CR spectrum above q_{inj} has a cooling time $\tau_{\text{cool}}(q_{\text{inj}}, \alpha_{\text{inj}})$ which equals the energy injection time-scale τ_{inj} defined as the ratio of the present CR energy to the energy injection rate (above q_{inj}). Therefore, we have

$$\tau_{\text{cool}} = \tau_{\text{inj}}, \text{ where} \quad (85)$$

$$\tau_{\text{cool}} = \tau_{\text{cool}}(q_{\text{inj}}, \alpha_{\text{inj}}) = \frac{\mathcal{E}_{\text{CR}}(\dot{C}_{\text{inj}}, q_{\text{inj}}, \alpha_{\text{inj}})}{(d\mathcal{E}_{\text{CR}}(\dot{C}_{\text{inj}}, q_{\text{inj}}, \alpha_{\text{inj}})/dt)_{\text{C+had}}}, \text{ and}$$

$$\tau_{\text{inj}} = \tau_{\text{inj}}(q_{\text{inj}}, \alpha_{\text{inj}}, C, q, \alpha) = \frac{\mathcal{E}_{\text{CR}}(C, q, \alpha)}{(d\mathcal{E}_{\text{CR}}(\dot{C}_{\text{inj}}, q_{\text{inj}}, \alpha_{\text{inj}})/dt)_{\text{inj}}}.$$

This leads to the condition

$$\tau_{\text{cool}}(q_{\text{inj}}, \alpha_{\text{inj}}) = \tau_{\text{cool}}(q, \alpha), \quad (86)$$

which indeed implies $q_{\text{inj}} = q$ in the case $\alpha_{\text{inj}} = \alpha$. In other cases one has to solve Eqs. (84) and (86) numerically for q_{inj} and q . The normalisation of the equilibrium CR spectrum can then be derived from Eq. (83) and is given by

$$C = Q_{\text{inj}} \tau_{\text{C}}(q, \alpha) \frac{T_{\text{p}}(q)}{T_{\text{CR}}(q, \alpha)} \frac{1 - \alpha}{1 - \alpha_{\text{inj}}} \frac{q_{\text{inj}}^{1-\alpha_{\text{inj}}}}{q^{1-\alpha}}. \quad (87)$$

The resulting spectra for $\alpha_{\text{inj}} = 2.5$ and $\alpha = 2.25, 2.5$, and 2.75 are displayed in Fig. 5.

4.1.3. Comparison of the spectra

Although Fig. 5 shows that the approximated and correct CR spectra are different in detail, their integral properties are very similar. The total energy in the approximated spectrum with $\alpha = \alpha_{\text{inj}} = 2.5$ is only 10% above the correct one, and the pressure difference is even smaller with 5%. Since the low energy part of the spectrum is ignored in our formalism, it is not surprising that the total CR number density is underestimated by 60%. Similarly, the Coulomb heating of the thermal background gas by the approximated CR spectrum seems to be underestimated by 80%. However, this is not correct, since in our formalism the CRs injected below the cutoff q return their energy instantaneously to the thermal gas. If one takes this into account one finds that the Coulomb heating rates agree with 1% accuracy. Since our description is energy conserving, this implies that the hadronic losses, and thereby the total hadronic induced radiation in gamma rays, electrons and neutrinos, agree also on a 1% level. However, the agreement of the differential radiation spectra at a given photon, electron or neutrino energy is worse ($\sim 10\% \dots 30\%$ overestimate), due to the different normalisation of the high energy part of the approximated and the correct CR spectra.

For comparison, we also calculate the accuracy of the matched asymptotic spectrum and equilibrium spectra of our formalism for spectral indices different from the injection index,

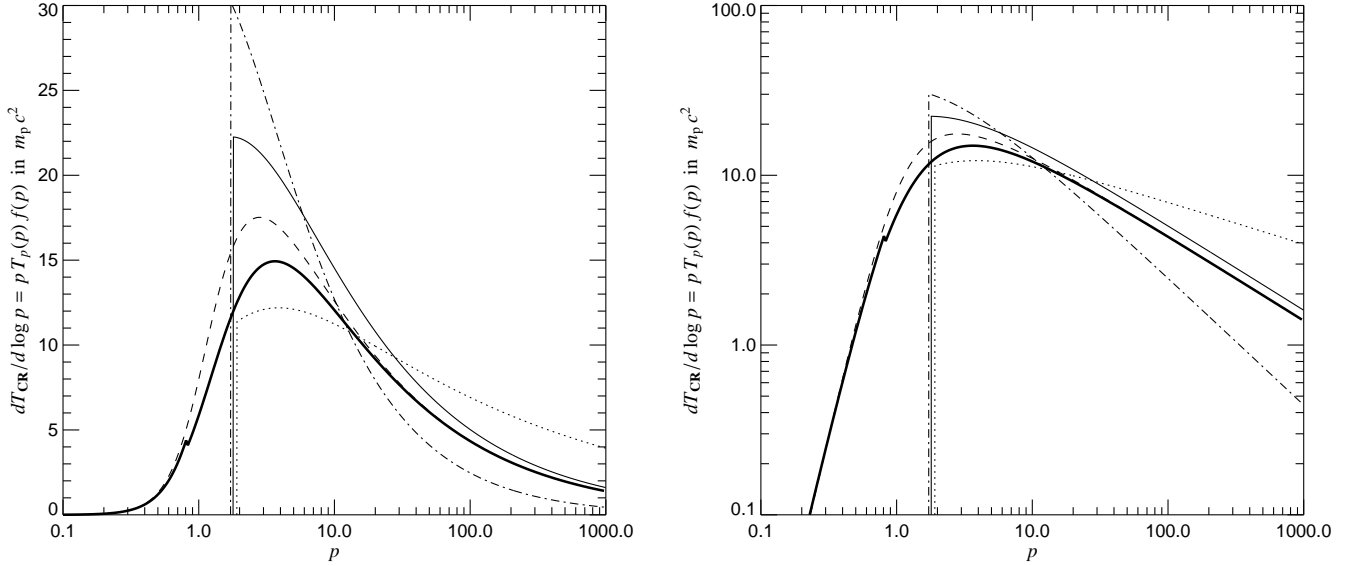


Fig. 5. Spectral energy distribution per logarithmic momentum interval of a steady state CR population within a volume element of our test system in log-linear (left) and log-log (right) representation. CRs are injected with an spectral index of $\alpha_{\text{inj}} = 2.5$. The thick line gives the correct spectrum of the full problem, the dashed line is the matched asymptotic solution, and the profiles with the low-momentum cutoff are equilibrium spectra in our formalism for the assumed spectral indices $\alpha = 2.25$ (dotted curve), $\alpha = \alpha_{\text{inj}} = 2.5$ (solid line), and $\alpha = 2.75$ (dash-dotted curve). The small bump at $p = 0.83$ in the correct spectrum is due to vanishing hadronic losses below this momentum. The areas under the curves in this plot are proportional to the CR energy, which differ less than 20% between approximate and accurate spectra (see Tab. 2).

Table 2. Relative accuracy of CR energy, pressure, number, and Coulomb loss rate in the various spectral approximations displayed in Fig. 5, compared to the numerical solution of the problem (also displayed in Fig. 5).

namely $\alpha = 2.25$ and $\alpha = 2.75$. The corresponding relative accuracies of CR energy, pressure, number, and Coulomb loss rates are similar and can be found in Tab. 2.

This demonstrates that, despite the roughness of the representation of the CR spectrum in our formalism, CR energy density and pressure are calculated with an accuracy acceptable for first exploration studies of the influence of CRs on galaxy and structure formation. The limitations of the approach, especially in representing the detailed spectral shape of the CR population, have also become clearer.

4.2. Freely cooling CR spectra

Setting the right-hand side in Eqn. (73) to zero describes the cooling of an initially injected spectrum. Fig. 6 shows the time evolution of numerically exact and approximate spectra with an initial condition described by $(C_0, q_0, \alpha) = (1, 10^{-3}, 2.5)$ and $(C_0, q_0, \alpha) = (1, 10^3, 2.5)$, respectively. The numerically exact spectra were obtained using the CR spectrum evolution code by Jasche et al. (2007, submitted). The approximative CR spectra were calculated using the implementation of the approximative CR evolution by Jubelgas et al. (2006). A fully ionized Hydrogen-only plasma with electron density of 1 cm^{-3} was assumed.

For timescales below the cooling time of $\sim 50 \text{ Myr}$ most of the spectral evolution happens in the low-energy cutoff, and the approximate treatment captures the evolution of the exact solution quite well. Both solution approach a similar asymptotic

shape, with a low energy cut off close to the trans-relativistic regime. However, the cooling rate seems to be different for the two descriptions, the approximate solution seems to cool on a slightly larger timescale. This inaccuracy is a consequence of the approximative description.

The momentum losses per hadronic interaction are lower for trans-relativistic particles than for ultra-relativistic particles. In our approximative description the ultra-relativistic particles benefit therefore from the reduced energy losses of the trans-relativistic CRs. This effect should therefore vanish for an ultra-relativistic-only CR spectrum. Indeed, as can be seen in the right panel of Fig. 6, as long as all CRs are ultra-relativistic, the approximative solution follows very closely the exact one.

To summarize, within one hadronic cooling time, the approximative spectral evolution is accurate if the correct spectral index is set. However, the long-term evolution of a freely cooling CR population becomes inaccurate after a few cooling times. This is the more the case the steeper the CR spectrum is. For applications where first order effects of the CR dynamics are considered, this level of accuracy should be sufficient. For applications which require a high level of accuracy over several cooling times a proper treatment of the spectral evolution would be needed. However, this is beyond the scope of this work.

5. Smoothed particle hydrodynamics

In this section, we describe how the dynamical effects of a CR population can be included into the smoothed particle hydrodynamics (SPH) simulation technique.

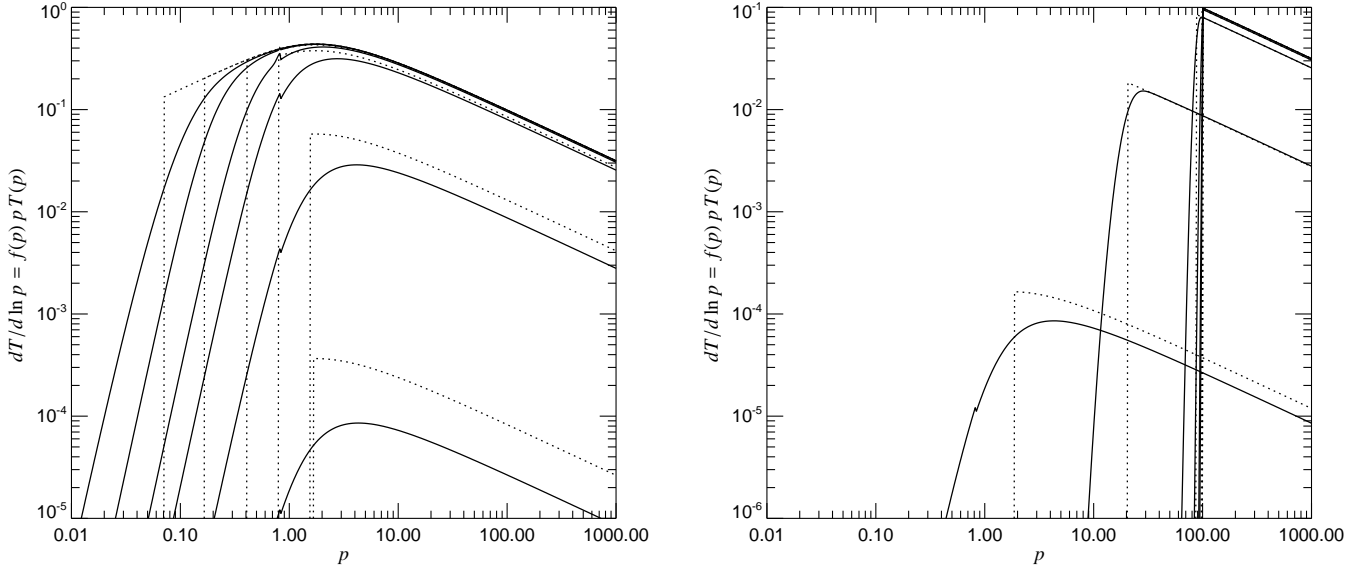


Fig. 6. Spectral energy distribution per logarithmic momentum interval of a freely cooling CR populations within a volume element of our test system. The initial CR populations are described by $(C_0, q_0, \alpha) = (1, 10^{-3}, 2.5)$ (left panel) and $(C_0, q_0, \alpha) = (1, 10^3, 2.5)$ (right panel). Spectra are shown for cooling ages of $\approx (0.01, 0.1, 1, 10, 100, 300)$ Myr. The numerically exact solutions are shown with solid lines. The approximative solutions are displayed by dotted lines.

5.1. Lagrangian fluid dynamics

The Lagrange density of a magneto-hydrodynamical gas-CR medium is

$$\mathcal{L}(\mathbf{r}, \dot{\mathbf{r}}) = \frac{1}{2} \rho \dot{\mathbf{r}}^2 - \varepsilon_{\text{th}}(\rho, A) - \varepsilon_{\text{CR}}(\rho, C_0, q_0) - \varepsilon_B, \quad (88)$$

where $\varepsilon_{\text{th}} = \rho A_0 (\rho/\rho_0)^{\gamma-1}/(\gamma-1)$ is the thermal energy density of a gas with adiabatic index γ and an entropy described by the adiabatic invariant A . Any adiabatic invariant $X \in \{A_0, C_0, q_0\}$ is simply advected with an adiabatic flow:

$$\frac{dX}{dt} = \left(\frac{dX}{dt} \right)_{\text{non-adiabatic}}, \quad (89)$$

where the rhs allows for non-adiabatic changes discussed in Sect. 3. The density evolves according to

$$d \ln \rho / dt = -\nabla \cdot \dot{\mathbf{r}}, \quad (90)$$

and the magnetic field according to the MHD-induction law:

$$\frac{\partial \mathbf{B}}{\partial t} = \nabla \times (\dot{\mathbf{r}} \times \mathbf{B} - \eta \nabla \times \mathbf{B}) \quad (91)$$

5.2. SPH formulation

In smoothed particle hydrodynamics (SPH), the fluid is discretised as an ensemble of particles which carry the mass, energy, and thermodynamic properties of the fluid elements. Macroscopic properties of the medium such as the density at position \mathbf{r}_i of the i -th particle are calculated with adaptive kernel estimation in the form

$$\rho_i = \sum_j m_j W(|\mathbf{r}_i - \mathbf{r}_j|, h_i), \quad (92)$$

where m_j is the mass of the j -th fluid element and $W(r, h)$ is the SPH smoothing kernel. The SPH particle positions \mathbf{r}_i are the dynamical variables of the simulation. However, following

the approach of Springel & Hernquist (2002) which we extend in this work to include an additional CR population and to allow for a general equation of state of the gas, the smoothing-kernel lengths h_i will be considered as dynamical variables of a Lagrangian function.

We introduce the CR spectrum of the i -th SPH particle

$$m_i \hat{f}_i(p) = m_i \frac{dN_{\text{CR}}}{dp dm} = \frac{m_i}{\rho(\mathbf{r}_i)} \frac{dN_{\text{CR}}}{dp dV} = \frac{m_i}{\rho(\mathbf{r}_i)} f_i(p) \quad (93)$$

with the help of the CR number per momentum and unit gas mass $\hat{f}_i(p)$. Our power-law template spectra are then described by

$$\hat{f}_i(p) = \hat{C}_i p^{-\alpha} \theta(p - q_i), \quad (94)$$

where $\hat{C}_i = C(\mathbf{r}_i)/\rho(\mathbf{r}_i)$ denotes the CR normalisation constant of the i -th SPH particle. Similarly, we introduce the CR energy, CR density, and thermal energy per unit gas mass with $\hat{\varepsilon}_{\text{CR}} = \varepsilon_{\text{CR}}/\rho$, $\hat{n}_{\text{CR}} = n_{\text{CR}}/\rho$, and $\hat{\varepsilon}_{\text{th}} = \varepsilon_{\text{th}}/\rho$, respectively. The equations defining these quantities and their changes due to adiabatic and non-adiabatic processes in terms of \hat{C} and q can be obtained from the corresponding formulae in this paper by replacing C with \hat{C} . For instance, Eqn. (4) yields

$$\hat{\varepsilon}_{\text{CR},i} = \int_0^\infty dp \hat{f}_i(p) T_p(p) = \frac{\hat{C}_i m_p c^2}{\alpha - 1} \times \left[\frac{1}{2} \mathcal{B}_{\frac{1}{1+q_i}^{\frac{\alpha-2}{2}}} \left(\frac{\alpha-2}{2}, \frac{3-\alpha}{2} \right) + q_i^{1-\alpha} \left(\sqrt{1+q_i^2} - 1 \right) \right], \quad (95)$$

and so on.

The Lagrange formalism provides an elegant way for deriving the equations of motions for SPH simulations. The SPH discretised Lagrangian is

$$\mathcal{L}(\mathbf{q}, \dot{\mathbf{q}}) = \sum_i \frac{m_i}{2} \dot{\mathbf{r}}_i^2 - \sum_i m_i \hat{\varepsilon}_i + \sum_i \lambda_i \phi_i, \quad (96)$$

where $\hat{\varepsilon}_i = \hat{\varepsilon}_{\text{th}} + \hat{\varepsilon}_{\text{CR}}$ is the total energy per mass of the i -th SPH particle, and $\mathbf{q} = (\{\mathbf{r}_i\}, \{h_i\}, \{\lambda_i\})$, which should not to be

confused with the CR spectral cutoff q , denotes all degrees of freedom of the system. These are the components of the SPH particle positions \mathbf{r}_i and the smoothing lengths h_i and their velocities. The λ_i s are Lagrange multipliers introduced by Springel & Hernquist (2002) in order to incorporate the choice of the smoothing length h_i into the Lagrangian via the function

$$\phi_i(\mathbf{q}) = \frac{4\pi}{3} h_i^3 \rho_i - M_{\text{SPH}}, \quad (97)$$

where M_{SPH} is the required mass within the smoothing kernel.

Here, we have ignored the description of magnetic fields within the SPH-Lagrangian. For the moment, we treat the evolution of the magnetic field separately from this Lagrangian formalism, adding instead the magnetic forces ad-hoc to the momentum equations of the SPH particles. This is along the lines of Dolag et al. (1999), and seems to work well in typical cosmological settings. However, we note that the dynamical influence of magnetic fields can in principle also be included into the SPH Lagrange-function as Price & Monaghan (2004a,b) demonstrate.

If one derives the SPH-equation of motion from a Lagrangian, one obtains a dynamical system which obeys energy and entropy conservation. Non-adiabatic processes, like shock waves, radiative energy losses and energy exchange of the thermal and relativistic fluids, thermal conduction, and CR diffusion have to be added into these equations. The way such process should be implemented in case of CR populations should become clear from this work.

5.3. Equations of motion

The equations of motions (of the adiabatic, non-magnetic part) of the SPH description follow from the Hamilton principle, namely

$$\frac{d}{dt} \frac{\partial \mathcal{L}}{\partial \dot{\mathbf{q}}} - \frac{\partial \mathcal{L}}{\partial \mathbf{q}} = 0. \quad (98)$$

The equation determining the smoothing length of the i -th particle follows from the variation of the action with respect to the Lagrange-multiplier λ_i . The corresponding part of the Euler-Lagrange equations yields

$$\phi_i = 0, \quad (99)$$

which for the special form chosen in Eqn. (97) leads to an implicit equation for h_i that has to be solved numerically in practice.

Variation with respect to h_i leads to an equation for λ_i :

$$\lambda_i = \frac{\partial \hat{\epsilon}_i}{\partial h_i} \left[\frac{\partial \phi_i}{\partial h_i} \right]^{-1} = \frac{\partial \hat{\epsilon}_i}{\partial \rho_i} \frac{\partial \rho_i}{\partial h_i} \left[\frac{\partial \phi_i}{\partial h_i} \right]^{-1}. \quad (100)$$

Using now Eqn. (97), one gets

$$\lambda_i = \frac{3 m_i}{4 \pi h_i^3} \frac{\partial \hat{\epsilon}_i}{\partial \rho_i} g_i, \quad \text{with } g_i \equiv \left[1 + \frac{h_i}{3 \rho_i} \frac{\partial \rho_i}{\partial h_i} \right]^{-1}. \quad (101)$$

Furthermore, the thermodynamical pressure is defined as

$$P = - \left(\frac{\partial E}{\partial V} \right)_S, \quad (102)$$

where $S = S_i$ denotes the entropy of a SPH particle volume element of size $V = V_i = \rho_i/m_i$ and internal energy $E = m_i \hat{\epsilon}_i$. This pressure definition can be used to express the derivative of

the SPH particle energy with respect to the local density in terms of the total (thermal plus CR) thermodynamical pressure:

$$\frac{\partial \hat{\epsilon}_i}{\partial \rho_i} = \frac{P_i}{\rho_i^2} = \frac{P_{th,i} + P_{CR,i}}{\rho_i^2} \quad (103)$$

One might argue that this derivation should only be correct for thermodynamic systems, and therefore not necessarily for CR populations which do not exhibit a Boltzmann distribution function. However, the concept of entropy, and the concept of adiabatic processes, which do not change phase space density and therefore leave entropy constant, is well defined for an arbitrary distribution function. Therefore, Eqn. (103) is a generally valid result, which can also be confirmed by an explicit calculation.⁷

Thus, the Lagrange-formalism for a variable SPH smoothing length introduced by Springel & Hernquist (2002) for a polytropic equation of state can easily be generalised to a general equation of state by replacing the thermal gas pressure by the total pressure of all fluid components. A calculation along the lines of Springel & Hernquist (2002) shows that the SPH-particle equations of motion read

$$\frac{d\mathbf{v}_i}{dt} = - \sum_j m_j \left[g_i \frac{P_i}{\rho_i^2} \nabla_i W_{ij}(h_i) + g_j \frac{P_j}{\rho_j^2} \nabla_j W_{ij}(h_j) \right], \quad (104)$$

with $\mathbf{v}_i = \dot{\mathbf{r}}_i$, $P_i = P_{th,i} + P_{CR,i}$ the thermal plus CR pressure, and $W_{ij}(h_i) = W(|\mathbf{r}_i - \mathbf{r}_j|, h_i)$.

6. Conclusion

We have introduced a simplified model for the description of cosmic ray physics with the goal of facilitating cosmological hydrodynamical simulations that self-consistently account for the dynamical effects of CRs during structure formation. We have shown how various adiabatic and non-adiabatic processes can be described in terms of a simple model for the local CR spectrum, consisting of a power-law with varying normalisation and low-energy cutoff. In our basic model, the CR spectral index is held fixed and chosen in advance to resemble a typical spectral index for the system under consideration. We have also described an extended model where the spectral index is allowed to vary as well, which leads to a numerically more involved scheme.

We have demonstrated that dynamical quantities like CR energy, pressure, and energy loss rates are all reasonable well represented by our approximative treatment of the CR spectra in case of a steady state situation in which CR injection and cooling balance each other. The accuracy is $\sim 10\%$ even if the spectral indices of CR injection and population do not match. Given the large uncertainties in our knowledge of the parameters determining the CR physics like CR injection efficiency, the level of accuracy of our numerical treatment seems to be sufficient. Thus, the formalism is suitable for explorations of the possible dynamical impact of CRs on galaxy and large-scale structure formation.

We have explained how our description of the CR physics can be self-consistently included into the SPH simulation methodology. The formulation we propose manifestly conserves energy and particle number. In particular, CR entropy is exactly

⁷ The internal energy per SPH particle of an ideal (thermal and/or relativistic) gas can be written as $m_i \hat{\epsilon}_i = m_i \sum_a \int dp \hat{f}_{a,i}(p) T_a(p)$, where a is the index over the particle species (electrons, protons, etc.) with momentum-space distribution functions $\hat{f}_{a,i}(p)$, and $T_a(p)$ the relativistic correct kinetic energy of the particles (Eqn. (5)). A straightforward calculation of $\partial \hat{\epsilon}_i / \partial \rho_i$, which uses the first equality in Eqn. (6), leads then to Eqn. (103).

conserved in adiabatic processes, and the dynamical forces from CR pressure gradients are derived from a variation principle.

This paper has outlined a basic framework for future work on the impact of CR populations on galaxy and large-scale structure formation. It is accompanied by two papers describing the implementation and testing of (i) the CR formalism as described here in the GADGET simulation code (Jubelgas et al. 2006), and (ii) a shock capturing method for SPH that allows on-the-fly estimation of the Mach number of structure formation shock waves, which is essential to follow CR injection accurately (Pfrommer et al. 2006). Further science applications are in preparation.

Appendix A: Numerically updating the CR spectrum

A.1. Constant spectral index

Updating the adiabatic invariant variables \hat{C}_0 and q_0 is most conveniently done via Eqn. (13) and (14). However, if the relative changes during a numerical time-step are large, e.g. due to rapid CR production at a location without a substantial initial CR population, these equations would have to be integrated on a refined time-grid, or solved with an implicit integration scheme. Both methods would be very time-consuming. Therefore, we propose another updating scheme: from the initial variables $\hat{C}_0(t_0)$ and $q_0(t_0)$ at time t_0 , the corresponding instantaneously particle number \hat{n}_{CR} , energy density $\hat{\epsilon}_{\text{CR}}$, and average particle energy T_{CR} are calculated according to Eqns. (2) to (5). Then \hat{n}_{CR} , $\hat{\epsilon}_{\text{CR}}$, and T_{CR} are updated using the non-adiabatic CR energy and number losses or gains during that time-step. And finally, these updated values have to be translated back into updated values of $\hat{C}_0(t_1)$ and $q_0(t_1)$. This is easiest by first inverting Eqn. (5) in order to calculate q , and then to use Eqns. (2) and (3) to get the updated $\hat{C}_0(t_1)$ and $q_0(t_1)$. The inversion of Eqn. (5) has to be done numerically for $T_{\text{CR}} \sim m_p c^2$, e.g. using pre-calculated numerical tables. However, for the asymptotic regimes we propose the following approximate inversion formulae:

$$q(\tau) = \begin{cases} q_a + \frac{q_a^{A-\alpha}}{(3-\alpha)\mathcal{B}}, & \tau = T_{\text{CR}}/(m_p c^2) \ll 1 \\ \frac{\alpha-2}{\alpha-1}(\tau+1), & \tau = T_{\text{CR}}/(m_p c^2) \gg 1 \end{cases}, \quad (\text{A.1})$$

$$\text{with } q_a = \left(\frac{2\tau}{\mathcal{B}}\right)^{\frac{1}{\alpha-1}}, \text{ and } \mathcal{B} = \mathcal{B}\left(\frac{\alpha-2}{2}, \frac{3-\alpha}{2}\right). \quad (\text{A.2})$$

A.2. Variable spectral index

If the relative changes of the dynamic CR variables \hat{C} , q , and α during a numerical time-step are large we propose the following numerically efficient updating scheme (instead of updating via Eqns. (15) and (16)): from the initial variables $\hat{C}_0(t_0)$, $q_0(t_0)$, and $\alpha(t_0)$ at time t_0 , the corresponding instantaneous particle number \hat{n}_{CR} , energy density $\hat{\epsilon}_{\text{CR}}$, and pressure \hat{P}_{CR} are calculated according to Eqns. (2) to (6). Then \hat{n}_{CR} , $\hat{\epsilon}_{\text{CR}}$, and \hat{P}_{CR} are updated according to the losses or gains of non-adiabatic CR energy, pressure, and number density during that time-step. And finally, these updated values have to be translated back into updated values of $\hat{C}_0(t_1)$, $q_0(t_1)$, and $\alpha(t_1)$. This can be done by numerically solving the following equation for the root q ,

$$\frac{P_{\text{CR}}}{n_{\text{CR}}} \frac{q^{1-\alpha(q)}}{\alpha(q)-1} = \frac{m_p c^2}{6} \mathcal{B}_{\frac{1}{1-\alpha(q)}} \left(\frac{\alpha(q)-2}{2}, \frac{3-\alpha(q)}{2} \right), \text{ and} \quad (\text{A.3})$$

$$\alpha(q) - 1 = \frac{3P_{\text{CR}}}{\epsilon_{\text{CR}} - T_p(q)n_{\text{CR}}}. \quad (\text{A.4})$$

These equations are obtained by combining Eqns. (3), (4), and (6). The new CR spectral index α and C are obtained by Eqns. (A.4) and (3).

Acknowledgements

We acknowledge helpful comments by Eugene Churazov and by an anonymous referee. We thank Jens Jasche for performing simulations of freely cooling CR spectra.

References

- Abramowitz, M. & Stegun, I. A. 1965, Handbook of mathematical functions (New York: Dover)
- Axford, W. I., Leer, E., & McKenzie, J. F. 1982, A&A, 111, 317
- Bell, A. R. 1978a, MNRAS, 182, 147
- Bell, A. R. 1978b, MNRAS, 182, 443
- Berezhko, E. G., Yelshin, V. K., & Ksenofontov, L. T. 1994, Astroparticle Physics, 2, 215
- Bieber, J. W. & Matthaeus, W. H. 1997, ApJ, 485, 655
- Blasi, P. 2002, Astroparticle Physics, 16, 429
- Blasi, P., Gabici, S., & Vannoni, G. 2005, MNRAS, 361, 907
- Brunetti, G., Blasi, P., Cassano, R., & Gabici, S. 2004, MNRAS, 350, 1174
- Brunetti, G. & Lazarian, A. 2007, ArXiv Astrophysics e-prints
- Cassano, R. & Brunetti, G. 2005, MNRAS, 357, 1313
- Cho, J. & Lazarian, A. 2004, ApJ, 615, L41
- Dermer, C. D. 1986a, ApJ, 307, 47
- Dermer, C. D. 1986b, A&A, 157, 223
- Dolag, K., Bartelmann, M., & Lesch, H. 1999, A&A, 348, 351
- Dolag, K. & Enßlin, T. A. 2000, A&A, 362, 151
- Drury, L. 1983, Space Science Reviews, 36, 57
- Drury, L. O., Markiewicz, W. J., & Völk, H. J. 1989, A&A, 225, 179
- Drury, L. O. & Voelk, J. H. 1981, ApJ, 248, 344
- Duffy, P., Kirk, J. G., Gallant, Y. A., & Dendy, R. O. 1995, A&A, 302, L21
- Eichler, D. 1979, ApJ, 229, 419
- Eilek, J. A. 1979, ApJ, 230, 373
- Enßlin, T. A. 2003, A&A, 399, 409
- Giacalone, J. & Jokipii, J. R. 1999, ApJ, 520, 204
- Gould, R. J. 1972, Physica, 58, 379
- Groom, D. R. & Klein, S. R. 2000, Rev. of Particle Physics, European Physical Journal C, 163, 379
- Hanasz, M. & Lesch, H. 2003, A&A, 412, 331
- Jones, T. W. & Kang, H. 1993, ApJ, 402, 560
- Jubelgas, M., Springel, V., Enßlin, T. A., & Pfrommer, C. 2006, submitted
- Kang, H. & Jones, T. W. 1995, ApJ, 447, 944
- Kang, H. & Jones, T. W. 2005, ApJ, 620, 44
- Kuwabara, T., Nakamura, K., & Ko, C. M. 2004, ApJ, 607, 828
- Longair, M. S. 1992, High energy astrophysics. Vol.1: Particles, photons and their detection (High Energy Astrophysics, by Malcolm S. Longair, pp. 436. ISBN 0521387736. Cambridge, UK: Cambridge University Press, March 1992.)
- Malkov, M. A., Diamond, P. H., & Völk, H. J. 2000, ApJ, 533, L171
- Malkov, M. A. & Völk, H. J. 1998, Advances in Space Research, 21, 551
- Malkov, M. A. & Völk, H. J. 1995, A&A, 300, 605
- Mannheim, K. & Schlickeiser, R. 1994, A&A, 286, 983
- Miller, J. A., Larosa, T. N., & Moore, R. L. 1996, ApJ, 461, 445
- Miniati, F. 2001, Computer Physics Communications, 141, 17
- Miniati, F., Ryu, D., Kang, H., & Jones, T. W. 2001, ApJ, 559, 59
- Narayan, R. & Medvedev, M. V. 2001, ApJ, 562, L129
- Pfrommer, C. & Enßlin, T. A. 2004, A&A, 413, 17
- Pfrommer, C., Springel, V., Enßlin, T. A., & Jubelgas, M. 2006, MNRAS, 367, 113
- Price, D. J. & Monaghan, J. J. 2004a, MNRAS, 348, 123
- Price, D. J. & Monaghan, J. J. 2004b, MNRAS, 348, 139
- Ptuskin, V. S., Moskalenko, I. V., Jones, F. C., Strong, A. W., & Mashnik, S. G. 2005, Advances in Space Research, 35, 162
- Rechester, A. & Rosenbluth, M. 1978, Phys. Rev. Lett., 40, 38
- Rybicki, G. B. & Lightman, A. P. 1979, Radiative processes in astrophysics (New York, Wiley-Interscience)
- Ryu, D. & Kang, H. 2003, Journal of Korean Astronomical Society, 36, 105
- Ryu, D. & Kang, H. 2004, Journal of Korean Astronomical Society, 37, 477
- Ryu, D., Kang, H., Hallman, E., & Jones, T. W. 2003, ApJ, 593, 599
- Schlickeiser, R. 2002, Cosmic ray astrophysics (Springer)
- Simpson, J. A. 1983, Annual Review of Nuclear and Particle Science, 33, 323

- Snodin, A. P., Brandenburg, A., Mee, A. J., & Shukurov, A. 2006, *MNRAS*, 373, 643
- Springel, V. & Hernquist, L. 2002, *MNRAS*, 333, 649
- Sternheimer, R. M. 1952, *Phys. Rev.*, 88, 851